



HAL
open science

Reductive catalytic depolymerization of industrial lignin and hemicellulose : process development and intensification

Xiaojia Lu

► **To cite this version:**

Xiaojia Lu. Reductive catalytic depolymerization of industrial lignin and hemicellulose : process development and intensification. Chemical and Process Engineering. Normandie Université; Åbo akademi, 2021. English. NNT : 2021NORMIR21 . tel-03588808

HAL Id: tel-03588808

<https://theses.hal.science/tel-03588808>

Submitted on 25 Feb 2022

HAL is a multi-disciplinary open access archive for the deposit and dissemination of scientific research documents, whether they are published or not. The documents may come from teaching and research institutions in France or abroad, or from public or private research centers.

L'archive ouverte pluridisciplinaire **HAL**, est destinée au dépôt et à la diffusion de documents scientifiques de niveau recherche, publiés ou non, émanant des établissements d'enseignement et de recherche français ou étrangers, des laboratoires publics ou privés.

Reductive catalytic depolymerization of industrial lignin and hemicellulose – process development and intensification

Xiaojia Lu



Åbo Akademi University
and Institut National des Sciences Appliquées de Rouen

2021



Xiaojia Lu

Born 1992, Shanxi, China

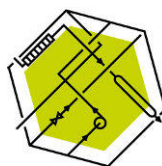
M. Sc. Environmental Engineering 2017
Chang'an University, Xi'an, Shaanxi, China

Reductive catalytic depolymerization of industrial lignin and hemicellulose – process development and intensification

Dépolymérisation catalytique réductrice de la lignine et de l'hémicellulose industrielles – développement et intensification des procédés

Reduktiv katalytisk depolymerisering av industriellt lignin och hemicellulosa – processutveckling och intensifiering

Xiaojia Lu



LSPC
Laboratoire
de sécurité
des procédés
chimiques

ISBN 978-952-12-4096-6 (printed version)/ ISBN 978-952-12-4097-3 (electronic version)
ISSN 2669-8315 2670-0638

Acta technologiae chemicæ Aboensia 2021 A/4

Painosalama, Turku/Åbo, Finland 2021

THESE

Pour obtenir le diplôme de doctorat

Spécialité Génie des Procédés

Préparée au sein de « l'Institut National des Sciences Appliquées de Rouen Normandie » et « Åbo Akademi University »

Reductive catalytic depolymerization of industrial lignin and hemicellulose – process development and intensification

Présentée et soutenue par
Xiaojia LU

Thèse soutenue publiquement le 1 octobre 2021 devant le jury composé de		
Ange NZIHOU	Professeur, IMT Mines Albi, France	Rapporteur
Ulla LASSI	Professeure, Oulun yliopisto, Finlande	Rapporteuse
Tapio SALMI	Professeur académique, Åbo Akademi University, Finlande	Examinateur
Carita KVARNSTRÖM	Professeure, Turun yliopisto, Finlande	Examinatrice
Mika HUUHTANEN	University Lecturer, Oulun yliopisto, Finlande	Examinateur
Lionel ESTEL	Professeur, LSPC, INSA Rouen, France	Co-Directeur de thèse
Henrik GRÉNMAN	Professeur, Åbo Akademi University, Finlande	Directeur de thèse
Sébastien LEVENEUR	MCF-HDR, LSPC, INSA Rouen, France	Directeur de thèse

Thèse dirigée par Sébastien LEVENEUR (INSA Rouen Normandie)
et Henrik GRÉNMAN (Åbo Akademi University)

To my family

“What's past is prologue”

- William Shakespeare

凡是过往 皆为序章

Preface

This work was carried out between 2017 and 2021 as a cotutelle (double degree) between Laboratoire de Sécurité des Procédés Chimiques (LSPC) of INSA Rouen Normandie (France) and Laboratory of Industrial Chemistry and Reaction Engineering (TKR) of Åbo Akademi University (Finland).

The China Scholarship Council is gratefully acknowledged for giving me the opportunity and financial support to complete this project. The Åbo Akademi University strategic profiling area Technologies for a Sustainable Future is also gratefully acknowledged for financial support.

I would like to express my sincere gratitude to my supervisors, Professor Sébastien Leveneur (LSPC), Professor Lionel Estel (LSPC) and Professor Henrik Grénman (TKR) for supervision of my doctoral studies and deep scientific discussions. I would like to acknowledge Professor Sébastien Leveneur who has chosen me among many candidates to execute this fantastic project. His rich knowledge, efficiency, patience, responsibility and enthusiasm have always inspired me over the past four years. His friend-like treatment made me feel at ease in a country 8000 kilometers away from home. I would like to thank Professor Lionel Estel for his great support, useful advice and insightful discussions, which have been important factors in shaping and guiding my work and allowed the project to proceed smoothly. I would like to express my gratitude to Professor Henrik Grénman for giving me the chance to carry out this cotutelle research. His excellent professionalism, extensive knowledge about biorefinery and perfect guidance helped me solve numerous complications and reach the preset goals of the thesis work in time. He could always find a good solution to many problems that I thought will never be solved.

I would like to express appreciation to our laboratory manager Kari Eränen for providing countless help on instrumentation, analysis, chemicals, etc. throughout my experiment. I would like to thank colleagues from Organic Chemistry, Lucas Lagerquist, Patrik Eklund and colleague from Wood and Paper Chemistry, Jarl Hemming for their help with analysis. I would like to thank Professor Johan Wärnå for his contributions on the kinetic modelling. I would like to thank Atte Aho, Jussi Rissanen, Paula Junghans, Stephanie Weckesser, Päivi Mäki-Arvela and Narendra Kumar for their assistants on my experimental study.

I am very grateful to all my colleagues in LSPC and TKR for their kindness and their great help to my work and life. I would like to specially thank Academy Professor Tapio Salmi and Professor

Dmitry Murzin for allowing me to work in the best ever laboratory and providing high-quality courses in the field of chemical engineering. Their enthusiasm and devotion to scientific research inspired and guided the strong academic atmosphere in the laboratory.

I feel very lucky to be surrounded by many friends. I deeply appreciate their company, support and inspiration. Xiaoshuang, Yanjun, Yuan, Jundong, Linlin, Xuelian, Yuzhen, Jie, Jing, Yanhong, Bojun, Xiaoyun, Wander, Soudabeh, Ananias, Ole, Pasi, Mark, Christoph, Mouad, Nemanja, Matias, Jussi, Ekaterina, Adriana, Zuzana, Jay Pee, Jogi, Rossana, Stephanie, Maria, Elizabeth, Jose, Chetna, Marie, thank you for being around and making my life better. I would like to specially thank Zepeng and Zuyi for their help with designing the cover of my thesis.

I would like to thank all jury members of my doctoral thesis defense: Ange Nzihou, Ulla Lassi, Tapio Salmi, Carita Kvarnström and Mika Huuhtanen for their time and availability for my defense.

Last but not least, I would like to thank my family. Thank you for your understanding and support. You are always the biggest motivation for my life and study.

Abstract

Modern biorefinery aims at utilizing renewable feedstocks to make a wide range of products such as chemicals, biofuels, and biomaterials while leaving as little residue as possible. Lignocellulosic biomass is a promising feedstock due to its availability, renewable nature, widespread application, and low competition with food. The fractionation of lignocellulose to its three main polymeric constituents and depolymerization of especially lignin and hemicellulose into monomers and oligomers before conversion into value-added chemicals is a key step in biorefineries. Despite a large potential, massive quantities of industrially produced hemicellulose and lignin are regularly simply burned for energy, which significantly hinders the realization of the sustainable bioeconomy. The current work is devoted to enhancing the depolymerization of lignin and hemicellulose fractions obtained from Finnish silver birch with the help of a novel semi-industrial method.

The lignin was depolymerized in different organic solvents or solvent mixtures under a hydrogen atmosphere in the presence of a heterogeneous catalyst. The goal was to acquire small aromatic compounds for further valorization. The influences of different parameters, including lignin solubility, reaction time, hydrogen pressure, reaction temperature, basic additives, type and loading of catalyst, as well as type and composition of organic/aqueous solvent on the kinetics was investigated. Selective and efficient depolymerization to monomers and dimers was achieved by process intensification.

The research on depolymerization of industrial hemicellulose was performed in two stages. The acidic hydrolysis of xylan to xylose was first studied in both batch and continuous reactors. Several commercial heterogeneous catalysts were screened, and the reaction parameters were optimized to find a compromise between the reaction kinetics of the hydrolysis and the undesired degradation of monosaccharide products to achieve the highest xylose yield. Moreover, the reaction kinetics was modelled successfully.

One flow through hydrolysis and hydrogenation of hemicellulose was investigated in a continuous reactor equipped with two catalyst beds. The xylose produced by hydrolysis was subsequently converted to xylitol in the second bed. The reaction temperature, hydrogen pressure

and residence time were varied to study the kinetics. A high yield (c. 90%) of xylitol was achieved and the kinetics was modelled obtaining a good fit to the experimental data.

The process of biomass valorization is typically highly temperature sensitive and it is not self-evident that isothermal processing conditions are optimal. The heat capacity of the reactor system is crucial when the process is performed under dynamic conditions and the heat capacity of catalyst support is not very well known and it was here studied in order to simulate and perform secure experimental operation in the future. The specific heat capacities of typical catalytic supports used in biorefinery applications were characterized with a Tian-Calvet micro-calorimeter. The temperature dependence was investigated for each catalytic material and polynomial expressions were successfully applied for simulating the experimental data. Significant differences were observed between the supports and the results contribute significantly to future development in valorization of biomass in dynamic conditions.

The current work contributes to the development and intensification of novel and sustainable processes for valorizing forest biomass according to the principles of green chemistry and process technology.

Résumé

La bioraffinerie moderne vise à utiliser des matières premières renouvelables pour fabriquer une large gamme de produits tels que des produits chimiques, des biocarburants et des biomatériaux tout en laissant le moins de résidus possible. La biomasse lignocellulosique est une matière première prometteuse en raison de sa disponibilité, de son aspect renouvelable, de son application généralisée et de sa faible concurrence avec le secteur alimentaire. Le fractionnement de la lignocellulose en ses trois principaux constituants polymères et la dépolymérisation de la lignine et de l'hémicellulose en particulier en monomères et oligomères avant la conversion en produits chimiques à valeur ajoutée est une étape clé dans les bioraffineries. Malgré un gros potentiel, des quantités massives d'hémicellulose et de lignine produites industriellement sont régulièrement simplement brûlées pour l'énergie, ce qui entrave considérablement la réalisation de la bioéconomie durable. Le travail actuel est consacré à l'amélioration de la dépolymérisation des fractions de lignine et d'hémicellulose obtenues à partir de bouleau verruqueux finlandais à l'aide d'une nouvelle méthode semi-industrielle.

La lignine a été dépolymérisée dans différents solvants organiques ou mélanges de solvants sous atmosphère d'hydrogène en présence d'un catalyseur hétérogène. L'objectif était d'acquérir de petites molécules aromatiques pour une valorisation ultérieure. Les influences de différents paramètres, y compris la solubilité de la lignine, le temps de réaction, la pression d'hydrogène, la température de réaction, les additifs basiques, le type et la charge du catalyseur, ainsi que le type et la composition du solvant organique/aqueux sur la cinétique ont été étudiées. Une dépolymérisation sélective et efficace en monomères et dimères a été obtenue par l'intensification du processus.

La recherche sur la dépolymérisation de l'hémicellulose industrielle a été réalisée en deux étapes. L'hydrolyse acide du xylane en xylose a d'abord été étudiée dans des réacteurs discontinus et continus. Plusieurs catalyseurs hétérogènes commerciaux ont été testés et les paramètres de réaction ont été optimisés pour trouver un compromis entre la cinétique de la réaction de l'hydrolyse et la dégradation indésirable des produits monosaccharidiques pour obtenir le rendement en xylose le plus élevé. De plus, la cinétique de la réaction a été modélisée avec succès.

Un processus consécutif d'hydrolyse et d'hydrogénation de l'hémicellulose a été étudié dans un réacteur continu équipé de deux lits catalytiques. Le xylose produit par hydrolyse a été converti en xylitol dans le second lit. La température de réaction, la pression d'hydrogène et le temps de séjour ont été modifiés pour étudier la cinétique. Un rendement élevé (c. 90 %) de xylitol a été obtenu et la cinétique a été modélisée avec succès.

Le processus de valorisation de la biomasse est généralement très sensible à la température et il n'est pas évident que les conditions de traitement isothermes soient optimales. La capacité thermique du système de réacteur est cruciale lorsque le processus est effectué dans des conditions dynamiques et la capacité thermique du support catalytique est très mal connue et cela a été étudié pour simuler et d'effectuer une opération expérimentale sécurisée à l'avenir. Les capacités thermiques spécifiques des supports catalytiques typiques utilisés dans les applications de bioraffinerie ont été caractérisées avec un micro-calorimètre Tian-Calvet. La dépendance à la température a été étudiée pour chaque matériau catalytique et des expressions polynomiales ont été appliquées pour simuler le comportement. Des différences significatives ont été observées entre les supports et les résultats contribuent de manière significative au développement futur de la valorisation de la biomasse en conditions dynamiques.

Cette thèse contribue au développement et à l'intensification de procédés nouveaux et durables pour valoriser la biomasse forestière conformément aux principes de la chimie verte et de la technologie des procédés verts.

Abstrakt

Moderna bioraffinaderier syftar på att använda förnybara råvaror för att producera ett brett sortiment av produkter så som kemikalier, biobränslen och biomaterial så att möjligast litet avfall uppstår. Lignosellulosa är ett lovande råmaterial på grund av stort utbud, förnybarhet, mångsidiga tillämpningsområden och för att den inte konkurrerar med livsmedelsproduktion. Nedbrytning av lignosellulosa till tre polymera huvudkomponenter och depolymerisering av speciellt lignin och hemicellulosa fraktionerna till monomerer och oligomerer före omvandling till värdeökade produkter är ett nyckelsteg i bioraffinaderier. Trots en stor potential förbränns en stor del av lignin och hemicellulosa inom den kemiska skogsindustrin för att producera värme och elektricitet, vilket inte stöder utveckling av hållbar bioekonomi. Denna avhandling syftar på kontrollerad och effektiv depolymerisering av lignin och hemicellulosa från finsk björk erhållen från en ny halvindustriell process genom att tillämpa processintensifiering.

Lignin depolymeriserades i olika organiska lösningsmedel under väteatmosfär i närvaro av heterogen katalysator. Målet var att erhålla monomerer eller små oligomerer för vidare uppgradering. Inverkan av olika processparametrar så som löslighet, tid, vätetryck, temperatur, pH, katalysator typ samt mängd och sammansättning av lösningsmedel på reaktionskinetiken undersöktes. Hög omsättningsgrad och selektivitet till monomerer och dimerer erhöles med hjälp av processintensifiering.

Forskningen i depolymerisering och valorisering av semi-industriell hemicellulosa genomfördes i två steg. Hydrolys av xylan till xylos i närvaro av syrakatalysator studerades i satsvisa och kontinuerliga reaktorer. Flera kommersiella heterogena katalysatorer undersöktes och processoptimering utfördes för att nå bästa möjliga balans mellan hydrolys och sönderfall av sockermonomererna för att uppnå en hög omsättning till xylos. Modellering av reaktionskinetiken utfördes med god framgång.

Konsekutiv hydrolys och hydrogenering av xylan till xylitol i en kontinuerlig reaktor utfördes i två seriekopplade katalysatorbäddar. Xylosen som producerades i första bädden blev direkt hydrogenerad till xylitol i den andra bädden. Temperaturen, vätetrycket samt uppehållstiden varierades för att optimera processen. Ett högt utbyte (c. 90%) till xylitol uppnåddes och kinetiken modellerades med framgång.

Valorisering av biomassa är typiskt mycket temperaturkänslig och det är inte självklart att isothermiska betingelser är de optimala. Värmekapaciteten av systemet är avgörande då processen utförs under dynamiska betingelser och värmekapaciteten av katalysatorns bärarmaterial är väldigt dåligt känd och detta studerades för att möjliggöra simuleringar och utförande av experiment på ett säkert sätt i framtiden. En Tian-Calvet-mikrokalorimeter användes för att systematiskt bestämma värmekapaciteten av vanliga bärarmaterial i olika temperaturer och polynomuttryck utvecklades för att simulera beteendet. Betydande skillnader upptäcktes och resultaten bidrar avsevärt till framtida utveckling av uppgradering av biomassa under dynamiska betingelser.

Denna avhandling bidrar till utveckling och intensifiering av nya hållbara processer för att valorisera skogsbiomassa enligt principerna för grön kemi och grön processteknik.

Curriculum Vitae

Xiaojia Lu

Born in 1992, Shanxi, China

Education

Oct. 2017-Sep. 2021 PhD candidate in chemical engineering (double degree)

LSPC, INSA Rouen & TKR, Åbo Akademi University

Sep. 2014-Jul. 2017 Master in Environmental Engineering

School of Environmental Science and Engineering, Chang'an University

Sep. 2010-Jul. 2014 Bachelor in Chemical engineering and technology

School of Environmental Science and Engineering, Chang'an University

Previous publications

1. Y. Li, **X. Lu**, J. Wu. *International Journal of Thermophysics*, 2016, 37: 16-29.
2. Y. Li, **X. Lu**, W. He, et al. *Journal of Chemical and Engineering Data*, 2016, 61: 475-486.
3. Y. Li, **X. Lu**, R. Huang, et al. *Journal of Chemical and Engineering Data*, 2016, 61: 2380-2390.
4. Y. Li, **X. Lu**, Q. Zhu, et al. *Fluid Phase Equilibria*, 2016, 430: 101-111.
5. Y. Li, **X. Lu**, Q. Luo, et al. *New Journal of Chemistry*, 2015, 39: 6223-6230.
6. Y. Li, Y. Gu, **X. Lu**. *Journal of Thermal Analysis and Calorimetry*, 2015, 122: 1455-1468.
7. Y. Li, Z. Xu, Q. Luo, **X. Lu**, J. Hu. *Thermochimica Acta*, 2016, 632: 72-78.
8. Y. Li, **X. Lu**, M. Zhang, et al. **Chinese Invention Patent**, 201310132333.5.
9. Y. Li, H. Li, **X. Lu**, et al. **Chinese Invention Patent**, 201310088853.0.
10. Y. Li, Q. Zhu, R. Huang, Y. Peng, **X. Lu**, et al. **Chinese Invention Patent**, 201410030061.2.

List of publications

- I. **X. Lu**, L. Lagerquist, K. Eränen, J. Hemming, P. Eklund, L. Estel, S. Leveneur, H. Grénman. Reductive catalytic depolymerization of semi-industrial wood-based lignin. *Industrial & Engineering Chemistry Research* (under review).
- II. **X. Lu**, P. Junghans, J. Wärnä, G. Hilpmann, R. Lange, H. Trajano, K. Eränen, L. Estel, S. Leveneur, H. Grénman. Hydrolysis of semi-industrial aqueous extracted xylan from birch (*betula pendula*) employing commercial catalysts – kinetics and modelling. *Journal of Chemical Technology & Biotechnology*, doi: 10.1002/jctb.6918. This manuscript has been accepted for publication.
- III. **X. Lu**, P. Junghans, S. Weckesser, J. Wärnä, G. Hilpmann, R. Lange, H. Trajano, K. Eränen, L. Estel, S. Leveneur, H. Grénman. One flow through hydrolysis and hydrogenation of semi-industrial xylan from birch (*betula pendula*) in a continuous reactor – kinetics and modelling. *Chemical Engineering and Processing - Process Intensification*, 2021, 169, 108614.
- IV. **X. Lu**, Y. Wang, L. Estel, N. Kumar, H. Grénman, S. Leveneur. Evolution of specific heat capacity with temperature for typical supports used for heterogeneous catalysts. *Processes*, 2020, 8, 911.

Authors contribution

- I X. Lu performed the experiments and wrote the manuscript; K. Eränen assisted with the experimental set-up; L. Lagerquist, J. Hemming and P. Eklund assisted with the analysis; H. Grénman, S. Leveneur and L. Estel supervised the experimental work and revised the manuscript.
- II X. Lu performed data analysis and wrote the manuscript; P. Junghans performed experiments and K. Eränen assisted with the experimental set-up; J. Wärnä and H. Trajano assisted with the modelling; G. Hilpmann and R. Lange assisted with the methodology; H. Grénman, S. Leveneur and L. Estel supervised the experimental work and revised the manuscript.
- III X. Lu performed a part of the experiments and wrote the manuscript; P. Junghans and S. Weckesser performed part of the experiments and K. Eränen assisted with the experimental set-up; J. Wärnä and H. Trajano assisted with the modelling; G. Hilpmann and R. Lange assisted with the methodology; H. Grénman, S. Leveneur and L. Estel supervised the experimental work and revised the manuscript.
- IV X. Lu performed the experiments and wrote the manuscript; Y. Wang assisted with the experiments; N. Kumar assisted with providing the support materials; S. Leveneur, H. Grénman and L. Estel supervised the experimental work and revised the manuscript.

Conference publications related to the topic

- I. **X. Lu**, L. Lagerquist, P. Eklund, S. Leveneur, L. Estel, H. Grénman. Reductive catalytic depolymerization of semi-industrial wood based lignin. 24th International Congress of Chemical and Process Engineering (CHISA), Prague, Czech Republic. March 2021. *Oral presentation*.
- II. **X. Lu**, H. Grénman, L. Estel, N. Kumar, S. Leveneur. Determination of the heat capacity of selected catalysts and catalyst supports. 24th International Congress of Chemical and Process Engineering (CHISA), Prague, Czech Republic. March 2021. *Poster presentation*.
- III. **X. Lu**, L. Lagerquist, P. Eklund, S. Leveneur, L. Estel, H. Grénman. Reductive catalytic depolymerization of semi-industrial wood based lignin. Finnish Young Scientist Forum on Catalysis (FYSFC 2021). April 2021. *Poster presentation*.

Table of contents

1 Introduction	1
1.1 Biorefinery	1
1.2 Biomass fractionation through a novel semi-industrial process.....	4
1.3 Reductive catalytic treatment of lignin and hemicellulose.....	6
1.3.1 Reductive catalytic depolymerization of lignin.....	6
1.3.2 Hydrolysis of hemicellulose	6
1.3.3 Hydrogenation of xylose	7
1.4 Specific heat capacity of heterogeneous catalysts.....	9
1.5 Aim and scope of the research	10
2 Experimental.....	13
2.1 Chemicals and materials.....	13
2.1.1 Lignin depolymerization	13
2.1.2 Xylan valorization	13
2.1.3 Specific heat capacity measurement.....	14
2.2 Experimental set-ups and procedures.....	16
2.2.1 Lignin depolymerization	16
2.2.2 Hydrolysis of xylan	17
2.2.3 Consecutive hydrolysis-hydrogenation of xylan	21
2.2.4 Specific heat capacity measurement.....	22
2.3 Characterization of products	25
2.3.1 Lignin depolymerization	25
2.3.2 Xylan valorization	26
3 Results	29
3.1 Reductive catalytic depolymerization of semi-industrial lignin.....	29
3.1.1 Solubility of the studied semi-industrial lignin	29
3.1.2 Influence of experimental parameters on reaction outcome.....	30
3.1.3 Lignin oil mass balance	40

3.1.4	Structural characterization of raw material and reaction products by NMR	41
3.1.5	Identification of lignin oil products by GC-MS	42
3.1.6	Characterization of different fractions from ultra-filtration	44
3.2	Catalytic hydrolysis of semi-industrial hemicellulose to monosaccharides in batch reactor	46
3.2.1	Catalyst screening.....	46
3.2.2	Influence of stirring speed.....	47
3.2.3	Influence of pH.....	48
3.2.4	Influence of temperature.....	49
3.2.5	Influence of particle size of the catalyst	50
3.2.6	Catalyst stability	51
3.2.7	Mathematical modelling.....	51
3.3	Catalytic hydrolysis of semi-industrial hemicellulose to monosaccharides in continuous reactor	57
3.3.1	Influence of pH.....	58
3.3.2	Influence of temperature.....	58
3.3.3	Influence of local pH.....	60
3.3.4	Residence time distribution	61
3.3.5	Mathematical modelling.....	64
3.4	One flow through hydrolysis and hydrogenation of semi-industrial hemicellulose to sugar alcohols in continuous reactor.....	67
3.4.1	Influence of temperature.....	68
3.4.2	Influence of flow rate	69
3.4.3	Influence of hydrogen pressure	70
3.4.4	Mathematical modelling.....	71
3.5	Specific heat capacity measurement for typical supports used for heterogeneous catalysts.....	74
4	Conclusions and perspectives	77
	Notation.....	81
	Acknowledgments.....	83
	References	85

1 Introduction

1.1 Biorefinery

With the rapid consumption of non-renewable resources, the increasing climate change and other environmental concerns, it is necessary to switch from a conventional fossil based economy to sustainable alternatives. The biorefinery concept [1] can be defined as a process or combination of processes for transforming biomass into various products such as biofuels, chemicals or materials [2].

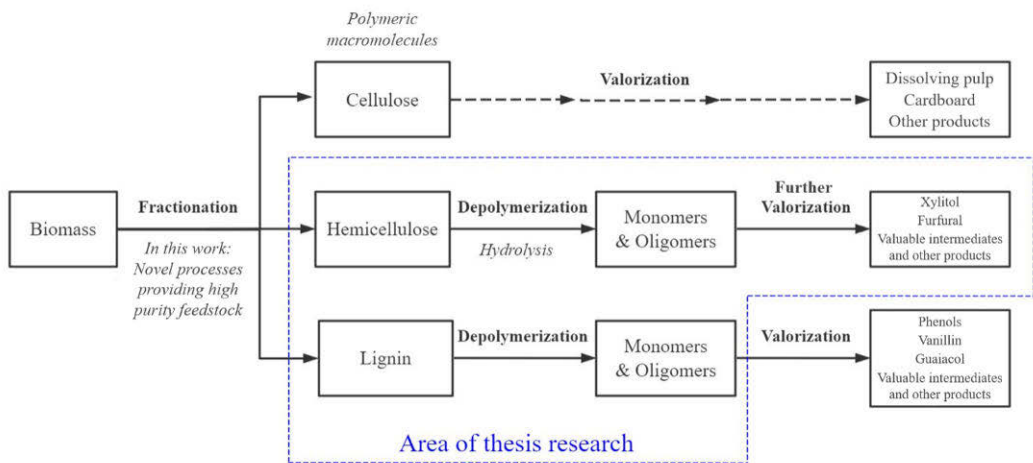


Figure 1. Conceptual representation of a possible biorefinery.

Lignocellulosic biomass is an abundant feedstock for biorefineries, covering a wide range of materials including non-wooden biomass, such as agricultural waste and woody biomass. Plant based biomass is estimated to be produced in 170-200 billion tons scale annually, of which 45-55% is cellulose, 25-35% hemicellulose, and 20-30% lignin [3]. The composition varies significantly based on species, origin, etc., and each of the polymers has varying levels of recalcitrance to fractionation and different potential for obtaining valuable end products [4].

Despite the highly significant potential, very large amounts of hemicellulose and lignin produced in industry is often simply combusted for energy production, which does not support taking full advantage of these valuable natural resources. Although energy can be required for operating the processes, utilizing at least a part of the lignin and hemicellulose for more value-added products

could provide a greener, more sustainable, and cost-competitive way for lowering greenhouse gas emissions, reducing fossil fuel reliance, and shifting toward a biobased economy [4].

Lignin, which constitutes up to 30% of all non-fossil organic carbon on earth, is rich in aromatic polymer components (Figure 2). It is a valuable renewable resource for novel biorefineries as it is a source of aromatic intermediates and fine chemicals, such as phenols, vanillin, guaiacol, eugenol, etc. [5,6], provided that efficient depolymerization technology exists. Lignin is produced in large quantities (> 300 billion tons) annually [7]. Nevertheless, it has led to limited industrial applications due to its recalcitrance towards valorization owing to the complex and varying molecular structure, broad molecular weight distribution and its tendency to undergo repolymerization and degradation during the lignocellulose fractionation [8].

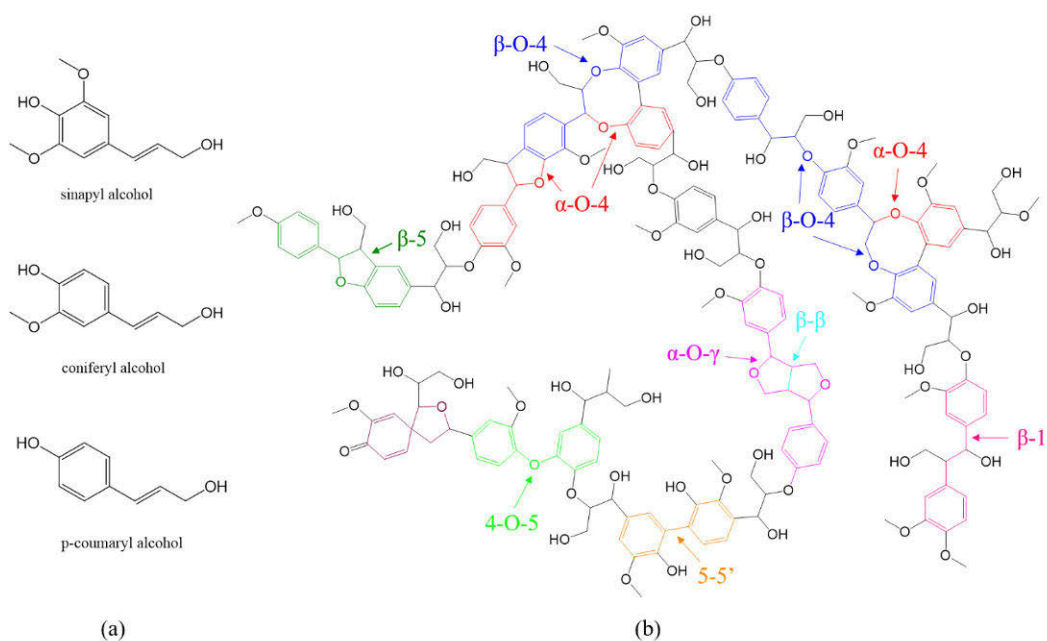


Figure 2. (a) Three phenylpropanol units in lignin; (b) the structure and main chemical linkages in lignin.

Three monolignol building blocks of lignin are presented in Figure 2(a). A 3D amorphous structure (molecular architecture) that contains a variety of bonds, of which typically 50% are β -O-4 bonds, is formed during lignification when the monolignols are linked by radical coupling. Other bonds, such as α -O-4, 5-5, β - β , 4-O-5, β -5 and β -1 are also formed, as shown in Figure 2(b).

1.2 Biomass fractionation through a novel semi-industrial process

The interest in utilizing different fractions of biomass has increased in recent years and substantial research on valorizing the whole biomass feedstock has been put forward. Hemicellulose, lignin and lignin-carbohydrate complexes extracted from biomass are the base for novel biorefinery applications, in addition to cellulose in its various forms. The pretreatment and further conversion of these bio-macromolecules to platform chemicals remains a significant challenge in current production, as versatile valorization methods already exist for the further conversion of e.g. sugars or lignin monomers.

Pretreatment is critical to the overall efficiency of a biorefinery process. The goal of the pretreatment is to fractionate the biomass into its three main components. The techniques employed should achieve highly efficient fractionation and retain their reactivity, while minimizing the generation of by-products that can even be inhibitory to the subsequent valorization processes. Moreover, it should naturally be cost-efficient. Pretreatment can be achieved through a single technology or a combination of technologies. Physical methods include process steps such as milling and grinding while physicochemical approaches include steam pretreatment/autohydrolysis, hydrothermolysis, and wet oxidation. Commonly utilized chemical methods treat the feedstock with either alkali, dilute acid, oxidizing agents or organic solvents. Other methods involve biological, or combinations of the methods.

An effective lignocellulosic biomass fractionation process has recently been developed, which generates three product streams [10,11]. A schematic diagram is shown in Figure 4. First, modified hot water extraction is applied to remove hemicelluloses from the birch chips (*betula pendula*) by extracting the polysaccharides from the fibrous wood structure in a heated water phase at 150°C and pressure below 8 bar. Then, almost all oxygen gas is eliminated to reduce the oxidation and degradation of hemicelluloses. The extraction is conducted under continuous recirculation to gain a purer and more concentrated hemicellulose fraction. The remaining chips are treated with sodium hydroxide (NaOH) to further separate lignin from cellulose fibers, producing black liquor rich in polymeric aromatic compounds. The black liquor is precipitated at pH 2.5, and then washed with acidified water to remove inorganics and water-soluble impurities. The lignin is then collected by filtration and dried.

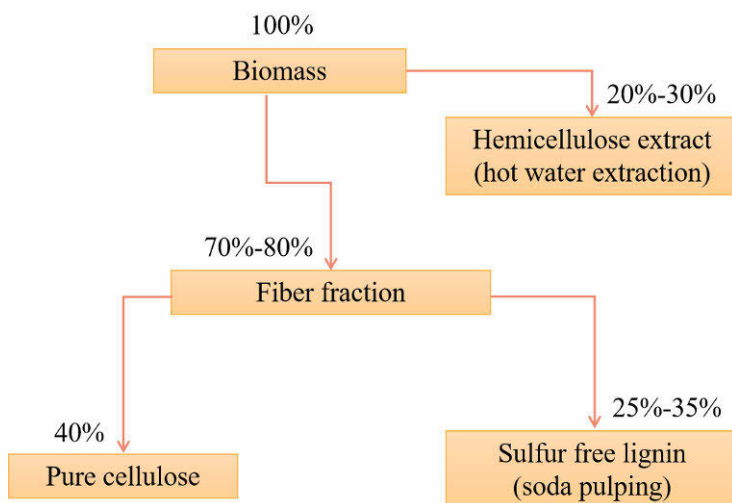


Figure 4. Schematic diagram of biomass fractionation through a new semi-industrial process.

This novel semi-industrial process efficiently isolates the hemicellulose and lignin from cellulose fibers, making it possible to utilize and add value to all the components. Almost pure hemicellulose is obtained after fractionation. The lignin produced has advantages such as sulfur-freeness, low carbohydrate content, and relatively high solubility in polar solvents. These features all contribute to the production of high-value products based on lignin.

1.3 Reductive catalytic treatment of lignin and hemicellulose

1.3.1 Reductive catalytic depolymerization of lignin

Reductive catalytic depolymerization (RCD) is a potential method for accomplishing efficient lignin depolymerization [12,13]. The lignin is processed in an organic solvent (or its aqueous mixture) under a reductive atmosphere with the help of a catalyst. Standard methods include mild hydroprocessing, harsh hydroprocessing, bifunctional hydroprocessing, and liquid-phase reforming. During the process, lignin is depolymerized by catalytic hydrogenolysis while repolymerization is notably hampered, which is attributed to the reductive stabilization of the reactive intermediates, producing a lignin oil rich in low molecular compounds.

1.3.2 Hydrolysis of hemicellulose

Acidic hydrolysis is a commonly employed approach for depolymerizing hemicelluloses, such as xylan, to provide monosaccharides [14]. The xylose produced is an important platform molecule, which can be valorized to, e.g. xylitol [14] or through furfural to a large variety of bio-chemicals for use in the paper, cosmetic, alimentary and pharmaceutical industries [15,16]. The general reaction mechanism of acidic hydrolysis of xylan is illustrated in Figure 5, in which the glycosidic bond is stepwise cleaved via protonation [17]. A mixture of oligomers and monomers with varying degrees of polymerization (DP) is typically produced when hemicelluloses are hydrolyzed. The oligomers can be further converted into monomers via either micro-biological, thermal, physio-thermal or chemical treatment. In addition, the monosaccharides may be dehydrated further in harsher conditions [18]. It is the formation of the covalent bonds between oxygen atoms of water and carbon atoms of polysaccharides that determines the rate of the reaction, a suitable catalyst can accelerate this process [19], whether it is homogeneous [20,21] or heterogeneous [22,23]. High monomer yields can be obtained in homogeneously catalyzed system, however, there is usually safety risks to the environment and the operators, as well as difficulties in developing efficient and inexpensive product separation processes [19]. Using heterogeneous catalysts can help in circumventing these problems. One of the drawbacks of heterogeneous catalysts is that mass transfer limitations can affect the reaction kinetics and lead to less efficient hydrolysis. The catalyst selection is crucial as the particle size, specific surface area, degree of cross-linking, porosity and many other characteristics can all affect the reaction progress. Moreover, performing the hydrolysis

under reductive conditions has the potential to suppress unwanted degradation of the obtained sugar monomers.

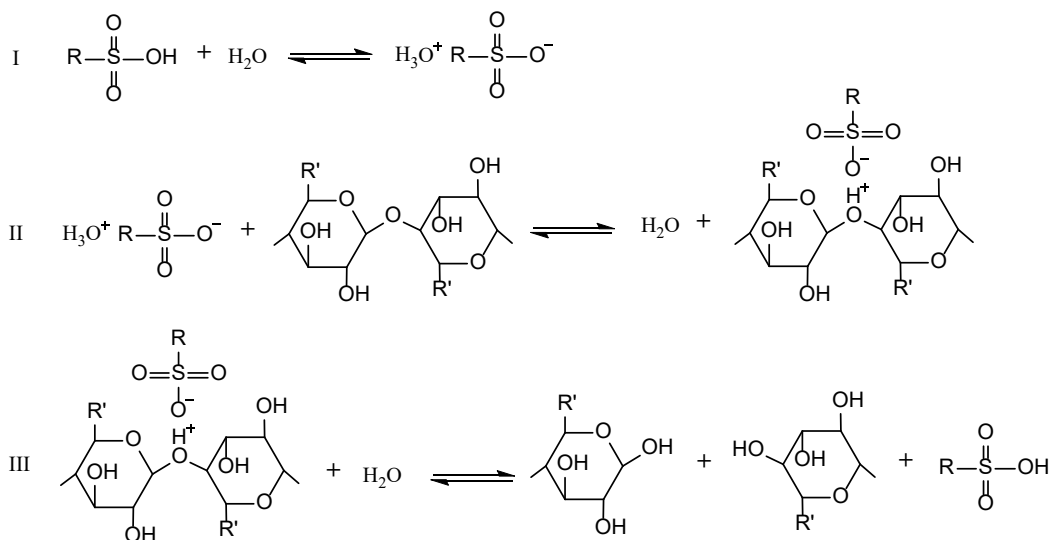


Figure 5. Reaction mechanism of acidic hydrolysis of xylan (R' = CH₂OH).

1.3.3 Hydrogenation of xylose

Xylitol is one of the most essential functional sugar alcohols in food, cosmetics, and pharmaceutical industries [24]. It is among the top 12 value-added biomass derived chemicals [25] and has become the most popular “natural” sweetener. Xylitol is primarily obtained via selective catalytic hydrogenation of naturally existed xylose performed either microbiologically or chemically.

In a typical chemical hydrogenation processing system, a solid catalyst is commonly utilized, along with hydrogen gas in order to obtain high atom efficiency [24]. Catalyst selection is essential for achieving high activity and selectivity towards xylitol production while avoiding deactivation by the fouling species. A variety of base and noble metal-based catalysts have been applied to the hydrogenation system, among which Raney nickel [22] has become a research hotspot for years because it is inexpensive, easy to use, highly active and selective. However, it usually undergoes fast deactivation, which accordingly affects the reaction kinetics and the product quality. Hydrogenation processes based on noble metals, such as platinum, palladium and ruthenium, have

also been actively studied, among which Ru-based catalysts have shown high activity and stability, showing great potential for being good alternatives for conventional Raney nickel catalysts [23].

1.4 Specific heat capacity of heterogeneous catalysts

Industrial processes are often performed under non-isothermal mode to, e.g., reduce energy consumption and lower the costs or influence selectivity. Non-isothermal conditions also enable continuous production with multi-step reactions as constant temperature is not always required. The design of non-isothermal processes involves calculating the mass and energy balances, where the thermodynamic properties of the reactants and catalysts play an important role, especially when considering large-scale production.

Heterogeneous catalysts have found wide application in industry also owing to their good hydrothermal stability, and reusability [26]. Commonly used catalytic materials and supports include zeolites, mesoporous materials, alumina, activated-carbon and resins. Research on characterization of these materials typically focus on measuring the morphology, particle size, specific surface area, porosity and acidity, etc. as they are important data for industrial applications. However, the heat capacities of catalysts are not typically reported in literature. This thermodynamic property varies significantly between different catalytic materials, which can influence the operation and temperature profile of a reactor system. Therefore, determining the specific heat capacity (C_p) of a catalyst is decisive for evaluating the thermal risk of a chemical process performed at non-isothermal mode especially when considering larger-scale production in continuous reactor systems with high catalyst loads and highly endo- or exothermic reactions involved. The data can be essential for modelling and simulation purposes, which builds the base for reliable design and operation of chemical processes.

Differential scanning calorimetry (DSC) has been widely utilized to measure heat capacities of different materials [27-29]. However, sensitivity of measurement and accuracy of correlation of the general DSC method are not always satisfactory. The methodologies of calibration and measurement also set high requirements for the samples, reactions, atmosphere, etc. The Setaram C80 3D Calvet Calorimeter has been designed as an alternative to conventional DSC equipments [30,31], but it provides higher accuracy.

1.5 Aim and scope of the research

The goal of this work was to develop and intensify heterogeneously catalyzed depolymerization of lignin and hemicellulose fractions obtained from a novel semi-industrial process for further valorization while keeping the reactivity of the products. Silver birch (*betula pendula*) was used as the biomass feedstock. Lignin macromolecules were aimed to be depolymerized to valuable aromatic compounds, which is still a serious bottleneck in current biorefinery production. Not only monomers but also short oligomers were aimed for as they also have potential for producing specialty chemicals. The aim was to achieve high yield while avoiding degradation of monomers and retaining their functional groups for enhancing further valorization. The hemicellulose fraction was subjected to an acidic hydrolysis process for monomer production. Commercial heterogeneous catalysts were screened and different reaction conditions were tested in order to achieve selective and efficient conversion for producing high yield of xylose and as few degradation products as possible. An aim was also to explore the possibility to develop a novel single pass through hydrolysis/hydrogenation of hemicelluloses. Moreover, another overall objective of this research was to contribute to the development of utilizing continuous reactors in the depolymerization of bio-macromolecules, as they are generally more efficient in industrial production. In order to enable future steps and designing efficient and safe processes in larger scale and continuous production, the specific heat capacity of heterogeneous catalytic materials commonly used in biomass valorization was studied.

A schematic representation of the research strategy is shown in Figure 6.

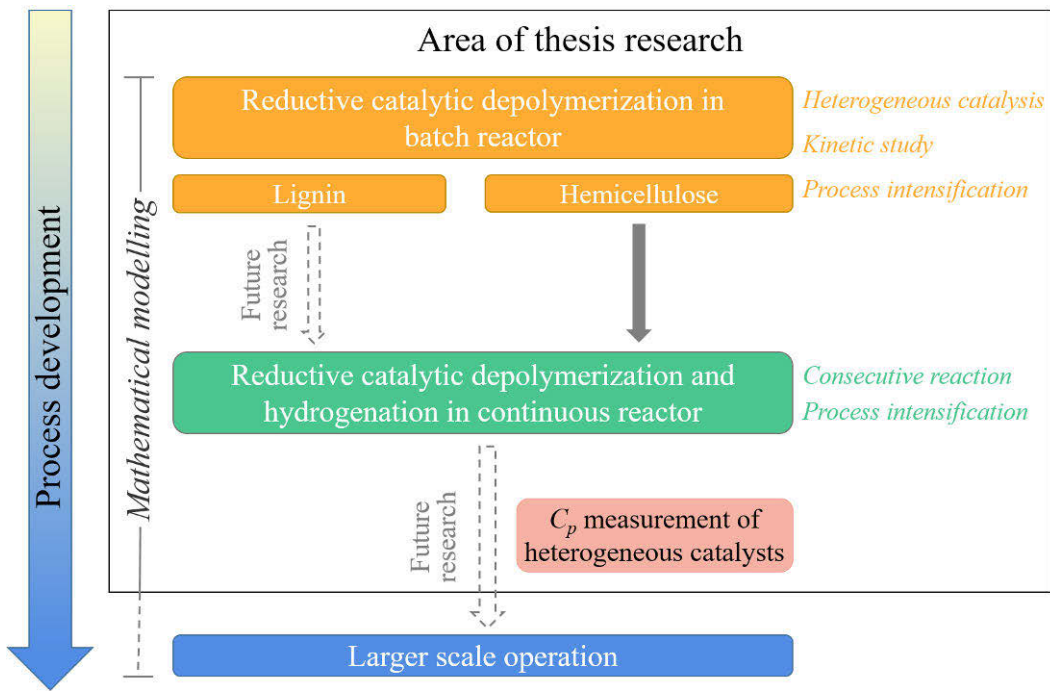


Figure 6. Research strategy of the doctoral thesis.

2 Experimental

2.1 Chemicals and materials

2.1.1 Lignin depolymerization

Ruthenium on carbon (5 wt%, Engelhard, Escat 40) was purchased from Engelhard Italiana S.p.A., Italy, the moisture of which was determined to be 46.75%. Ni/Al₂O₃ (5 wt%) was synthesized in the laboratory via a deposition-precipitation method and palladium on carbon (MKCK3216, 5 wt%) was obtained from Sigma Aldrich. All other chemicals were purchased from commercial suppliers and utilized without further purification.

Lignin, originating from Finnish silver birch, was obtained from a novel extraction aqueous-based process described in Section 1.2. Lignin from this process typically contains less than 2% of impurities, of which the main one is carbohydrates. More detailed analysis of this semi-industrial lignin material can be found in the work performed by Lagerquist et al. [32]. The lignin was used as obtained without further purification or separation.

2.1.2 Xylan valorization

Five heterogeneous catalysts were chosen for acidic hydrolysis of xylan based on their wide application and strong acidity. As supplied, the particle sizes of three selected catalysts (Amberlite IR120, Amberlyst 15 and Dowex 50WX8-50) are as close as possible. Smopex 101 is a non-porous fiber catalyst supplied in one diameter. The Dowex 50WX2-100 was chosen as comparison as it has a significantly lower degree of crosslinking. All tested catalysts are strong acids containing sulfonic acid groups and the mechanism of acidity is Brønsted acids. Ru/C was chosen for hydrogenation of xylose according to its previous performance of catalytic hydrogenation of monosaccharides. The basic information of these catalysts were listed in Table 1.

The semi-industrial xylan, produced by the same process as lignin, was selected as the starting material of the hydrolysis and consecutive hydrolysis-hydrogenation experiments. It was used as obtained without further purification or separation.

The total dissolved solid in the xylan solution was determined to be 38.8%. It has an average molecular weight (M_w) of 4.649 kg/mol, corresponding to a DP of around 31 assuming an average

monomer molar mass of 150.13 g/mol and 100% xylose in the substrate. The sugar composition has been analyzed by GC, as listed in Table 2, in which xylose is the main component in the substrate (79.3%).

Table 1. Information about the chosen catalysts.

Catalyst	Matrix	Moisture wt%	Particle size μm	Temp. max. $^{\circ}\text{C}$	TEC meq/g
Amberlite IR120	styrene-divinylbenzene (gel)	45	620-830	120	4.4
Amberlyst 15	styrene-divinylbenzene (macroreticular)	5	600-850	120	4.7
Dowex 50WX2- 100	styrene-divinylbenzene (gel)	78	149-297	150	4.8
Dowex 50WX8- 50	styrene-divinylbenzene (gel)	55	300-1180	150	4.8
Smopex 101	styrene sulfonic acid grafted polyolefin fiber	6	-	120	2.6
Engelhard 0.7% Ru/C	Activated carbon	-	355-500	-	-

Table 2. Composition analysis of the semi-industrial xylan.

Compo und	Arabi- nose	Xy- lose	4-O- Me- GlcA	Glucuro- nic acid	Galac- tose	Man- nose	Glu- cose	Rham- nose	Galac- turonic acid	Total
wt%	1.8	79.3	9.3	0.5	3.7	2.0	1.8	2.4	1.8	100

2.1.3 Specific heat capacity measurement

Eleven heterogeneous catalytic materials/supports were chosen for the C_p measurement since they are commonly used in industry. Their basic information was listed in Table 3. All materials were received or synthesized with high purities ($\geq 99\%$), and used without further purification.

Table 3. Information about the chosen catalytic materials.

	Type	Physical Form	SiO ₂ /Al ₂ O ₃ (mol/mol)	Manufacturer
Activated carbon	activated carbon	powder	-	Chemviron
Al ₂ O ₃	aluminum oxide	powder	-	Acros Organics
Amberlite IR120, H-form (53–58% moisture)	Ion-exchange resin	bead	-	Acros Organics
H-Beta-25	zeolite	powder	25	Zeolyst International
H-Beta-38	zeolite	powder	38	Zeolyst International
H-Y-60	zeolite	powder	60	Alfa Aesar
H-ZSM-5-23	zeolite	powder	23	Zeolyst International
H-ZSM-5-280	zeolite	powder	280	Zeolyst International
SiO ₂	silicon dioxide	powder	-	Merck
TiO ₂	titanium dioxide	pellet	-	Degussa
Zeolite 13X	zeolite	powder	1.8	Fluka

2.2 Experimental set-ups and procedures

2.2.1 Lignin depolymerization

The reductive catalytic depolymerization of lignin was conducted in a 300 mL Parr reactor with an overhead mechanical stirrer, as shown in Figure 7. A water/glycol cooling bath was connected to the reactor to perform sampling during the experiments by condensing the volatile products.

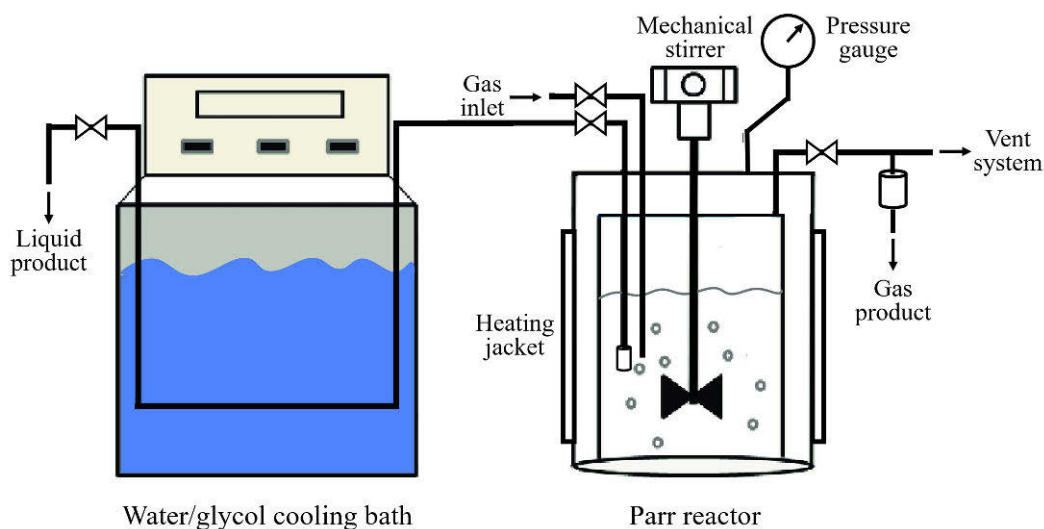


Figure 7. Schematic diagram of batch reactor system for reductive catalytic depolymerization of lignin.

Typically, 150 mL of pre-dissolved lignin solution, 0.8 g 5% Ru/C on the dry base were loaded into the reactor. The reactor was sealed and flushed first with argon and then hydrogen several times, followed by being pressurized to 20 bar with H₂ at ambient temperature. The system was rapidly heated to the desired temperature. The stirring was commenced at a constant speed of 1000 rpm upon reaching the desired temperature, which was set as time 0. The experiment lasted for 24 hours and intermediate samples were taken at regular intervals to monitor the reaction progress. A sinter was installed to the end of the sampling tube to avoid the loss of catalyst while taking samples. The intermediate samples were filtered with 0.45 μm PTFE filters to remove catalyst as well as possible undissolved lignin, followed by being dried and stored for analysis. After 24 hours experiments, the reactor was cooled to room temperature. Gas samples were taken and analyzed

with GC-FID/TCD before the reactor was carefully depressurized and disassembled. The liquid product was filtered and rinsed by adding additional solvent. The filtrate was collected, transferred to a rotary evaporation to dry, ready for subsequent analysis. In the experiments aimed at studying the mass balance, intermediate samples were not taken, instead only the final liquid and gaseous samples were collected. The yield of lignin oil was calculated with the following equation:

$$\text{Yield of lignin oil} = \frac{\text{weight of lignin oil (g)}}{\text{weight of lignin (g)}} \times 100\% \quad (1)$$

After selected experiments, the reaction mixture was introduced to a Millipore ultra-filtration system. A regenerated cellulose membrane with a pore size of 1 kDa was employed. The solvent-resistant stirred cell was sealed and pressurized to 4.75 bar with N₂, after which the stirring was started at a speed of 265 rpm. The ultra-filtration was carried out at ambient temperature. After the ultra-filtration, the filtrate was collected and dried for analysis. The residue consisting of larger lignin-derived molecules and catalyst was diluted to 150 mL using the same solvent and transferred back to the batch reactor to conduct a further oxidation experiment under 5 bar O₂ and 240°C.

2.2.2 Hydrolysis of xylan

2.2.2.1 Batch experiments

A 300 mL reactor was employed for the batch experiments, equipped with a four-blade mechanical impeller stirrer to achieve efficient mixing and reduce the influence of external mass transfer on the reaction kinetics. A sinter was installed to the end of the sampling tube to avoid the loss of catalyst while taking samples.

The catalyst was used as received without drying prior to experiments. The moisture content of the catalyst was taken into account when calculating the pH (apparent proton concentration) and the concentration of the substrate. The amount of catalyst was calculated with Equations 2 and 3, employing the total ion exchange capacity ($TEC_{dry\ cat.}$) listed in Table 1. The initial xylan concentration was calculated via Equations 4-7.

$$m_{dry\ cat.} = \frac{c_{H^+} V_{total}}{TEC_{dry\ cat.}} \quad (2)$$

$$m_{\text{wet cat.}} = \frac{m_{\text{dry cat.}}}{1 - \text{moisture content}\%} \quad (3)$$

$$m_{\text{water in cat.}} = m_{\text{wet cat.}} - m_{\text{dry cat.}} \quad (4)$$

$$V_{\text{solution}} = V_{\text{total}} - V_{\text{water in cat.}} \quad (5)$$

$$m_{\text{xylan}} = V_{\text{solution}} \times c_{\text{xylan}}^0 \quad (6)$$

$$c_{\text{xylan}} = \frac{m_{\text{xylan}}}{V_{\text{total}}} \quad (7)$$

Typically, 150 mL of xylan solution and a certain amount of catalyst were loaded to the reactor. The heating was started after the reactor was sealed and pressurized to 2 bar with argon. The first sample was taken after reaching the desired temperature, the stirring was then commenced. Samples were taken every half an hour with the outlet flushed before sampling. Argon was used for obtaining an inert atmosphere and regulating the overall pressure. The pressure was kept constant (8 bar) during the process until the reaction mixture was cooled down after 4 hours.

The xylan conversion and xylose yield were calculated as follows.

$$X_{\text{xylan}} = \frac{c_{\text{xylan}}^0 - c_{\text{xylan}}}{c_{\text{xylan}}^0} \times 100\% \quad (8)$$

$$Y_{\text{xylose}} = \frac{c_{\text{xylose}}}{c_{\text{xylan}}^0} \times 100\% = \frac{c_{\text{xylose}}}{c_{\text{xylan}}^0 \times x_{\text{xylose}}} \times 100\% \quad (9)$$

where c_i^0 and c_i represent the initial concentration of component i in the substrate and its concentration at the determined time, respectively. x_{xylose} denotes the content of xylose in the substrate, which is 79.3%.

2.2.2.2 Continuous experiments

The continuous experiment on xylan hydrolysis was carried out in a tubular reactor with upstream flow, as shown in Figure 8. The tube was surrounded by two external heaters and an aluminum jacket to obtain a uniform heating. The xylan solution was pumped into the reactor and the flow rate was adjusted for achieving desired residence time according to Equation 10. A heat

exchanger was installed after the reactor to cool down the liquid before sampling. In addition, an extra valve was utilized to ensure a constant pressure while taking samples.

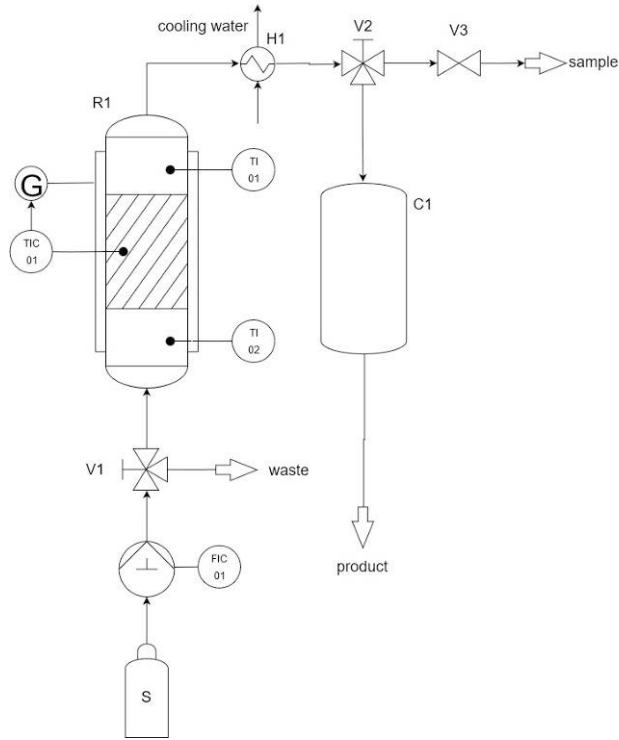


Figure 8. Reactor set-up for xylan hydrolysis.

The total reactor volume ($V_{reactor}$) was approximate 24 mL. The free volume in the catalyst bed (V_{liquid}) after filling was calculated to be 12 mL according to Equations 11-14.

$$\dot{V} = \frac{V_{liquid}}{\tau} \quad (10)$$

$$V_{reactor} = \left(\frac{d}{2}\right)^2 \times \pi \times L \quad (11)$$

$$m_{quartz} = V_{reactor} \times \rho_{b,quartz} \quad (12)$$

$$V_{quartz} = m_{quartz} \times \rho_{quartz} \quad (13)$$

$$V_{liquid} = V_{reactor} - V_{quartz} \quad (14)$$

The schematic diagram of the continuous reactor was shown in Figure 9. The catalyst bed was made up of quartz and catalyst. The ratio between quartz and catalyst was determined by the required pH (apparent proton concentration), while maintaining the catalyst amount identical. Accordingly, the length of the catalyst bed varied depending on the pH values.

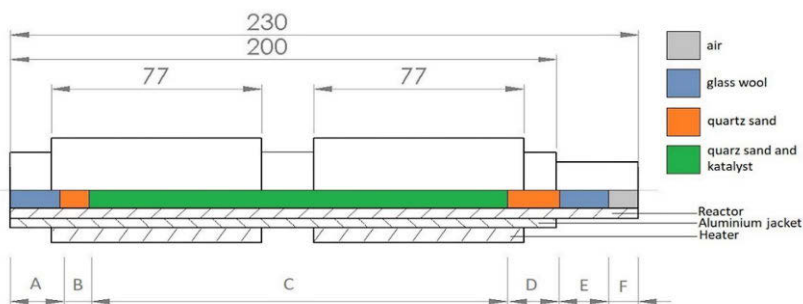


Figure 9. Schematic diagram of continuous reactor filling.

Two different proton concentrations were tested, corresponding to pH 0.3 and 0.5, respectively, assuming that all protons are free from the sulfonic groups. The catalyst amount was calculated with Equations 2 and 3, while the V_{total} in the equation was replaced by V_{liquid} . The details about reactor filling were illustrated in Table 4.

Table 4. Reactor filling for different apparent proton concentrations.

$c_{H^+,apparent}$	mol/L	0.513	0.316
A	cm	1.7	1.7
B	cm	1.0	1.0
C	cm	8.1	13.0
D	cm	6.9	3.0
E	cm	2.8	2.8
F	cm	2.5	1.5
$V_{reactor}$	cm ³	15.681	25.167
m_{quartz}	g	21.953	35.234
V_{quartz}	cm ³	8.284	13.296
V_{liquid}	cm ³	7.397	11.871
$m_{dry\ cat.}$	g	0.791	0.791
$m_{wet\ cat.}$	g	3.593	3.593

A 2 g/L xylan solution was utilized as substrate. The reactor was flushed with water during the heating process. The water was replaced by the xylan solution as soon as the desired temperature was reached, which was set as time 0. The first sample was taken after four times the residence time. Additional samples were taken to check whether the steady-state was obtained at constant temperature. The samples were filtered with 0.45 μm PVDF filters prior to analysis by different chromatographic methods. The xylan conversion and xylose yield was calculated with Equations 8 and 9 based on the analytical results.

2.2.3 Consecutive hydrolysis-hydrogenation of xylan

A tubular stainless steel reactor with a smaller diameter was employed to study the consecutive hydrolysis and hydrogenation of semi-industrial xylan in one flow through, as shown in Figure 10.

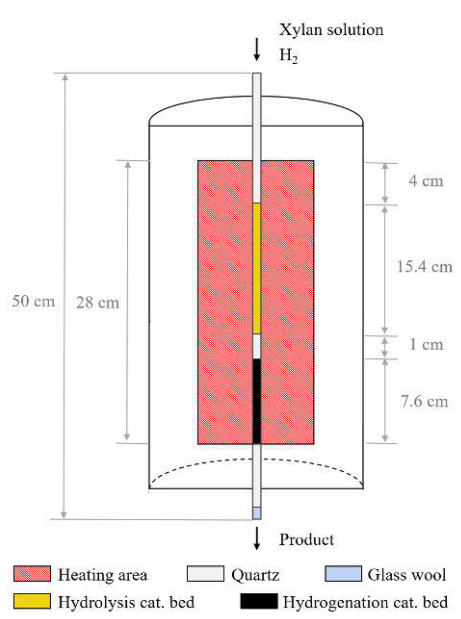


Figure 10. Schematic diagram of continuous reactor for consecutive hydrolysis-hydrogenation of xylan.

The reactants, i.e., xylan solution and H₂, were both fed from the top of the tube, followed by sequentially flowing through the hydrolysis catalyst bed and the hydrogenation catalyst bed, and finally collected at the bottom of the tube with a sampling pump. Dowex 50WX2-100 was mixed with quartz to build the hydrolysis catalyst bed according to the satisfactory results obtained in

xylyan hydrolysis experiments. The further hydrogenation of monosaccharides was catalyzed by 0.7% Ru/C. A heating jacket with a total heating length of 28 cm was installed to supply an evenly distributed heat. The pressure was kept constant during the whole process. The samples were collected with a sampling pump and filtered with 0.45 μm PVDF filters prior to analysis.

The xylitol yield was calculated based on the xylose composition in the substrate according to the following equation.

$$Y_{xylitol} = \frac{c_{xylitol}}{c_{xylose}^0} \times 100\% = \frac{c_{xylitol}}{c_{xylyan}^0 \times x_{xylose}} \times 100\% \quad (15)$$

where c_i^0 and c_i represent the initial concentration of component i in the substrate and its concentration at the determined time, respectively, and $x_{xylose} = 79.3\%$.

2.2.4 Specific heat capacity measurement

A C80 Tian–Calvet calorimeter (Figure 11), manufactured by Setaram instrumentation, equipped with a pair of Hastelloy reversing mixing cells, were applied to measuring the specific heat capacity of different catalytic materials in a temperature range of 313–453 K. The twin cells (Figure 11(c)) were surrounded by thermocouples and external thermal interferences in the calorimetric system has been eliminated by a differential coupling of the measurement and reference detectors, ensuring a precise determination of the heat flow. The standard error of the temperature measurement is 0.1 K and the enthalpy measurement 0.1%.

The measurement by C80 is carried out in a similar way as DSC, i.e., the difference in energy between the measured and the reference substances is measured under a programmed temperature control. Nonetheless, a caloric efficiency of up to 94% can be achieved, which is significantly higher than a typical plate DSC. In addition, the detector adopts a 3D full-clad calorimetric method, and, contrary to the general DSC, the heat flow inside the sample itself is taken into account during calorimetry. The measurement by C80 is independent of the weight, form, and nature of the sample, the measuring cell utilized, the manner of contact between sample and sensor, and the properties of sweeping gas, promising an excellent precision even for irregular-shaped samples or uneven heat conduction. Moreover, the temperature changes are well controlled, which leads to a more accurate C_p measurement.

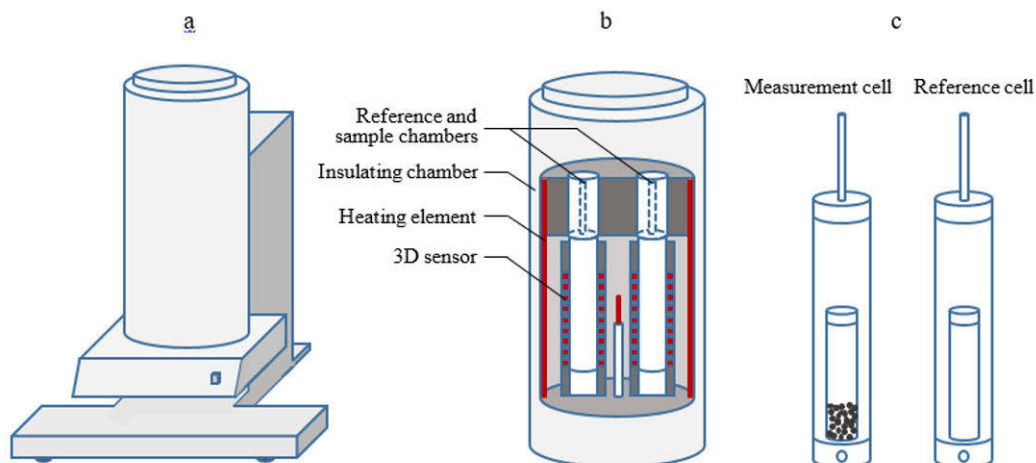


Figure 11. (a) General view of the C80 micro-calorimeter; (b) the heating block showing the geometry for the reference and measurement cells; (c) the Hastelloy reversing mixing cells and their contents.

Theoretically, the specific heat capacity is calculated based on the heat flow signal. The sample was dried overnight at 393 K, followed by being placed in the measurement cell at a certain amount, while the reference cell was kept empty (Figure 11(c)). The system was then sealed, and the heating was commenced according to the following temperature program: After heating to the first set-point (313 K), the twin cells were stabilized for 8400 s before increasing the temperature by 2 K at a speed of 0.5 K/min. During the heating process, the change in heat flow was recorded with the Setsoft 2000 software. The system was then kept isothermal for 4200 s, followed by being heated to the next set-point (333 K) at a speed of 1 K/min, and then stabilized for 8400 s. The steps were repeated until the heat flow variation at the last set-point (453 K) was recorded. The C_p measurement on each catalytic material was repeated 3 times without replacing the sample in between, giving a maximum standard error of 1.79%.

Figure 12 illustrated an example of the evolution of heat flow and temperature at a set-point (333 K) in a series measurement, where the heat flow signals represented the difference in heat flow between the measurement and reference cells with (blue) and without (red) loading a sample. The difference between the enthalpies of the two cells, i.e., the energy absorbed by the sample, was calculated by integrating the heat flow peak. The value was corrected by subtracting the data obtained in the blank measurement according to Equation 16.

2.3 Characterization of products

2.3.1 Lignin depolymerization

2.3.1.1 Analysis of gaseous products

The composition of gaseous products was determined by a gas chromatography equipped with a J&W GS-Q PLOT column (30 m × 0.53 mm). The front detector was a flame ionization detector (FID), utilized mainly for determining hydrocarbons, while the back detector was a thermal conductivity detector (TCD) for inorganic gases. The peaks were identified by GC-MS.

2.3.1.2 Analysis of lignin oil products

Molecular weight distribution

The molecular weight distribution of the lignin substrate and lignin-derived products was determined by high-pressure size-exclusion chromatography (HPSEC) utilizing two different methods, employing either an (A) Agilent 1100 Series HPLC instrument equipped with a G1315B DAD-detector or a (B) Shimadzu HPLC instrument equipped with an LT-ELSD detector. 2 × Jordi Gel DVB 500A (300 mm × 7.8 mm) columns + guard column (50 mm × 7.8 mm) in series were utilized in both systems. The analysis was performed at 40°C with 1 vol% acetic acid in tetrahydrofuran (THF) as eluent at a flow rate of 0.8 mL·min⁻¹ with 35 min analysis time/sample. The samples were prepared by dissolving dry lignin samples in THF to 1 mg/mL. The samples were then vortexed and filtered with a 0.45 μm PTFE filters. The peaks of monomers, dimers, trimers, and tetramers could be approximately quantified in the chromatogram according to the retention times of standard materials (syringaldehyde, hydroxymatairesinol, etc.). for example, the retention times for lignin monomer and dimer were determined to be 25.2 min and 22.2 min, respectively.

Quantitative GC analysis

The lignin oil products was quantitatively characterized using gas chromatography equipped with an FID detector and an Agilent J&W HP-1/SIMDIST column (6–7 m × 0.530 mm, film thickness 0.15 μm). The carrier gas was H₂ and the injection volume was 0.5 μL. Initial injector

temperature was 80°C (0.1 min) with a temperature rise at 50°C/min up to 110°C and then at 15°C/min to the final temperature of 330°C (7 min). The initial oven temperature was 100°C (0.5 min) with a temperature rise of 12°C/min up to 340°C (5 min), also the detector temperature was 340°C. The samples were mixed with certain amount of internal standard (kolesterol, 0.02 mg/mL) before silylation by (pyridine: N,O-bis(trimethylsilyl)trifluoroacetamide: chlorotrimethylsilane = 1: 4: 1). The peaks were identified by GC-MS by comparing them with an in-house spectral database.

NMR Spectroscopy

All the NMR experiments were performed at 25°C in DMSO-d₆ on an AVANCE III spectrometer (Bruker Biospin GmbH, Rheinstetten, Germany) operating at 500.13 MHz for ¹H and 125.77 MHz for ¹³C and 202.46 MHz for ³¹P. HSQC experiments used Bruker's pulse program "hsqcedetgpsisp2.3" for multiplicity edited with a spectral width of 8012 Hz (from 3.3–12.7ppm) and 20750 Hz (from 7.5–157.5 ppm) for the ¹H- and ¹³C-dimensions. The residual solvent peak was used as the internal reference $\delta_{\text{H}}/\delta_{\text{C}}$ (2.50/39.52 ppm). A common standard protocol was utilized for ³¹P NMR sample preparation [5].

2.3.2 Xylan valorization

HPLC

Two different HPLC methods were employed for the quantitative analysis of xylan-derived products. (A) A VWR Hitachi Chromaster HPLC equipped with a 5450 refractive index detector (RI). A Bio-Rad Aminex HPX-87C column (300 mm × 7.8 mm) was used. The eluent (1.2 mmol/L CaSO₄ solutions) was pumped into the column at a flow rate of 0.5 mL/min and a constant temperature of 80°C. (B) A Hewlett Packard series 1100 HPLC equipped with a Bio-Rad Aminex HPX-87H column and a RI detector. The analysis was performed at 45°C under isocratic conditions and a flow rate of 0.6 mL/min. The eluent consisted of 5 mmol/L H₂SO₄ solutions. Samples were filtered with 0.45 μm PVDF filters prior to injection. The calibration curves were determined by preparing a series of calibration samples with pure chemicals in the range of 0.31-5 g/L.

GC-FID

An Agilent J&W GC, model PeriknEmler Clarus 500, equipped with a 7.2 m × 0.530 mm column was employed. The carrier gas was hydrogen at a flow rate of 7 mL/min. The injection volume was 0.5 µL. The injector had an initial temperature of 80°C. After 0.1 min of injection, the temperature was increased by 50°C/min up to 110°C and afterward 15°C/min to 330°C. This temperature was kept stable for 7 min. The oven was heated at 100°C for 0.5 min and the temperature was then increased at 12°C/min up to 340°C for 5 min. An FID detector was used with 45 mL/min hydrogen and 450 mL/min air at 340°C. The samples were freeze-dried overnight and diluted to 1 g/L with distilled water. Cholesterol was added as the internal standard. The solutions were then silylated with (Pyridine: N,O-Bis(trimethylsilyl)trifluoroacetamide: Trimethylsilyl chloride = 1:4:1) prior to injection.

3 Results

3.1 Reductive catalytic depolymerization of semi-industrial lignin

Part of this chapter is adapted from the following article:

X. Lu, L. Lagerquist, K. Eränen, J. Hemming, P. Eklund, L. Estel, S. Leveneur, H. Grénman. Reductive catalytic depolymerization of semi-industrial wood-based lignin.

Technical lignin obtained from pulping industry are usually highly condensed and the reactivity is greatly reduced after treatment with different technologies, making it difficult to be efficiently used for platform molecule production. Herein a new lignin material produced by an extraction aqueous-based process, which has many advantages over traditional technical lignin, e.g., Kraft lignin, was introduced to a depolymerization system performed under reductive atmosphere. Different heterogeneous catalysts were screened and the experimental conditions varied to explore the influence of different parameters on the reaction kinetics. 1000 rpm was chosen as it has lead to much faster kinetics in previous experiments. All solid particles were determined to be well dispersed and there was high turbulence at 1000 rpm with the experimental set-up. Some of the experiments were repeated three times and the relative standard deviation was determined to be within 0.5-4.5%.

3.1.1 Solubility of the studied semi-industrial lignin

The solubility of lignin in THF at room temperature was tested to have a basic understanding of the characteristics of this novel semi-industrial wood-based lignin. The average value of solubility was determined to be 8.76 mg/mL, which was much higher than the values of other lignin materials, such as kraft lignin, whose solubility in THF was 1.44 mg/mL [33]. Lignin solubility generally decreases with condensation, which at least partly explains the difference.

The solubility of lignin in the reaction medium (1 g in 150 mL EtOH-H₂O (50/50, v/v)) under reaction conditions was also determined by performing non-catalytic experiments under otherwise

identical conditions as the RCD experiments. It can be concluded that the solubility of lignin increased with temperature and the lignin was completely dissolved in the EtOH-H₂O mixture at determined temperature (240°C) and initial H₂ pressure (20 bar). Correspondingly, the solubility decreased during the cooling process. However, the solubility was observed to be lower than that obtained at the same temperature during the heating process. This is probably caused by the repolymerization of lignin fragments during the whole measurement process.

3.1.2 Influence of experimental parameters on reaction outcome

3.1.2.1 Catalyst screening

Three different heterogeneous catalysts (Ru/C, Pd/C and Ni/Al₂O₃) were tested by adding an equivalent amount of each (dry basis) to the reactor while keeping the reaction conditions identical. As shown in Figure 13, the kinetics was observed to be faster in the beginning, followed by a slowing down of the depolymerization rate. This was most likely due to the varying reactivity of the different types of bonds in the lignin, among which some were cleaved faster, e.g., β-O-4 and α-O-4, some were cleaved slower, and some were not cleaved at all, e.g., possible C-C bonds. The cleavage slowed down when there were less reactive bonds in the reaction mixture. The use of Pd/C resulted in the fastest kinetics; however, ethane, propane and butane were observed in significant amounts in the gas phase, indicating a significant undesired cleavage of the aliphatic side chains of the lignin molecules [34], which was shown to be less severe employing other catalysts. It was observed, that RCD reaction with Ru/C was slightly slower, but the final mono- to tetramer yield (weight percentage in lignin oil products) of about 77% was similar to the yield obtained with the other two catalysts after 24 hours. In addition, the experiment catalyzed by Ru/C produced less polymers, showing a higher yield towards smaller aromatic compounds (mono- and dimers). Ni/Al₂O₃ also performed rather well, however, Ru/C was chosen due to the good performance and low acidity, since acidity typically leads to repolymerization of the lignin fragments.

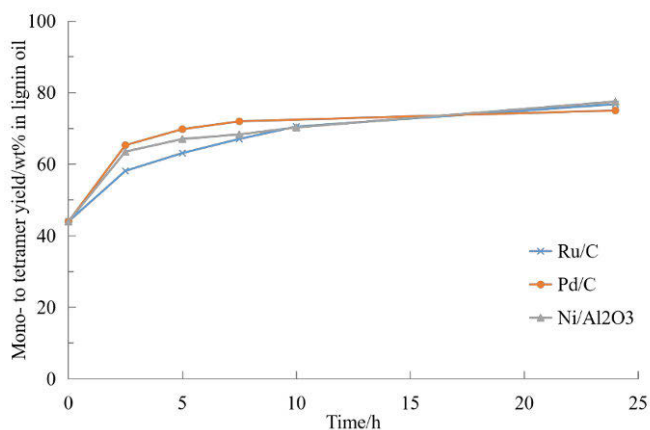


Figure 13. Effect of catalyst type on the mono- to tetramer yield in experiments performed in EtOH-H₂O (50/50, v/v) under 20 bar H₂ and 240°C.

3.1.2.2 Effect of sampling and pre-dissolution of lignin

A water/glycol cooling bath was installed to condense volatile compounds in gas phase during sampling, enabling investigating the evolution of the RCD process. To study if the sampling during the experiments influenced the lignin oil products, experiments with and without taking intermediate samples were performed under identical conditions. The results demonstrated that sampling during the experiment did not influence the lignin products in the liquid phase.

The influence of loading the lignin as solid or pre-dissolved solution (24 hours prior to the experiment) was explored. The experiments were carried out under otherwise identical reaction conditions, and the same amount of lignin was utilized as solid and in the solution. The results confirmed that the 24 hours pre-dissolution did not influence the depolymerization kinetics.

3.1.2.3 Effect of the presence of only H₂ or the catalyst

The effect of the presence of solely H₂ or the catalyst was investigated and compared to a blank experiment and the substrate, as displayed in Figure 14. The lignin oil produced by experiments performed without Ru/C or H₂ were observed to be much more condensed than the sample from a typical RCD reaction. The presence of the catalyst was observed to have a more significant effect

on the final product than H₂. This is most probably due to the fact that the solvent acted as a hydrogen-donor under inert atmosphere [35,36], which enabled hydrogenation without the introduction of gas phase hydrogen. Nonetheless, a significant difference was observed between the final product of the non-catalytic experiment under H₂ atmosphere and the substrate, which was confirmed by a mono- to tetramer yield of 62%., indicating the occurrence of non-catalytic reactions and/or thermal degradation.

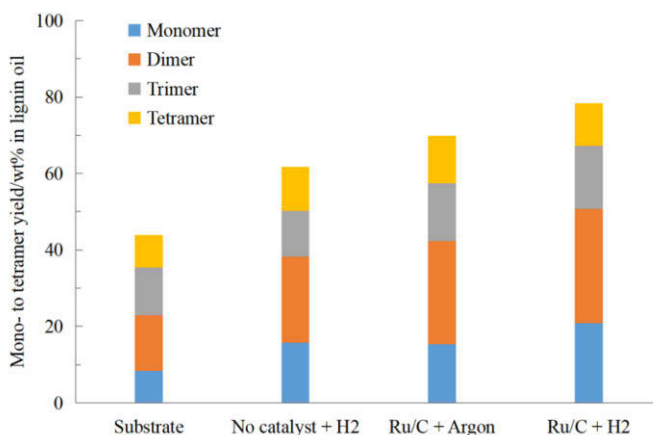


Figure 14. Effect of the presence of H₂ and catalyst on the mono- to tetramer yield after a 24 hours experiment in EtOH-H₂O (50/50, v/v) mixture at 240°C compared to a blank experiment with only substrate.

3.1.2.4 Influence of solvent on kinetics and mechanism

The intermediate samples taken during the experiments conducted in MeOH-H₂O (30/70, v/v) and EtOH-H₂O (50/50, v/v) were characterized by different methods, and the results are shown in Figures 15 and 16. The ratios of organic solvent to water in the reaction mediums were decided according to the maximum operating pressure of the batch reactor. It was observed that low molecular weight compounds were formed with time, whereas the proportion of polymers in the product mixture decreased. The final mono- to tetramer yield after 24 h experiment was determined to be 77% for the experiment conducted in EtOH-H₂O mixture and 98% in MeOH-H₂O mixture under the studied conditions (240°C and 20 bar hydrogen), indicating that the lignin polymers were efficiently cleaved into smaller compounds as the experiments proceeded. Smaller molecules than

aromatic monomers were not detected in the liquid product, which confirmed that the lignin monomers were not degraded during the experiments.

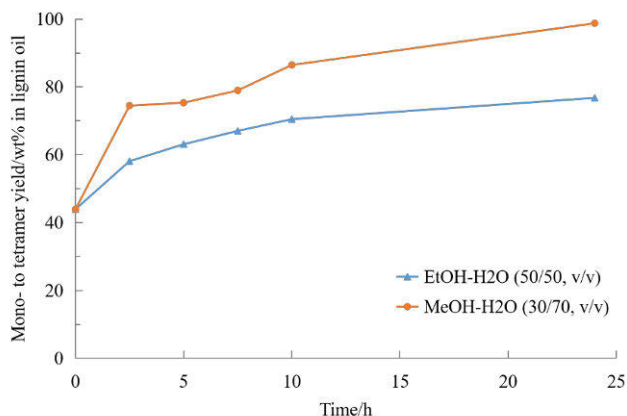


Figure 15. The mono- to tetramer yield as a function of time for experiments performed in MeOH-H₂O (30/70, v/v) and EtOH-H₂O (50/50, v/v) mixtures catalyzed by 5% Ru/C under 20 bar H₂ and 240°C.

Figure 16 showed the yield of mono-, di-, tri-, and tetramer as a function of time. When comparing with the results in Figure 15, it can be concluded that consecutive reactions occurred. The lignin macromolecules were first cleaved into oligomers, which then degraded to form dimers and monomers. This is especially evident in experiment conducted in MeOH-H₂O (30/70, v/v) (Figure 16b), where the conversion of oligomers to dimers and monomers was obviously more efficient in methanol-water mixture than ethanol-water mixture. Moreover, the changes in the slopes corresponding to monomer yields and dimer yields indicated the decrease in the reaction rate as the concentration of the most reactive bonds, e.g., β -O-4 and α -O-4, decreased with time.

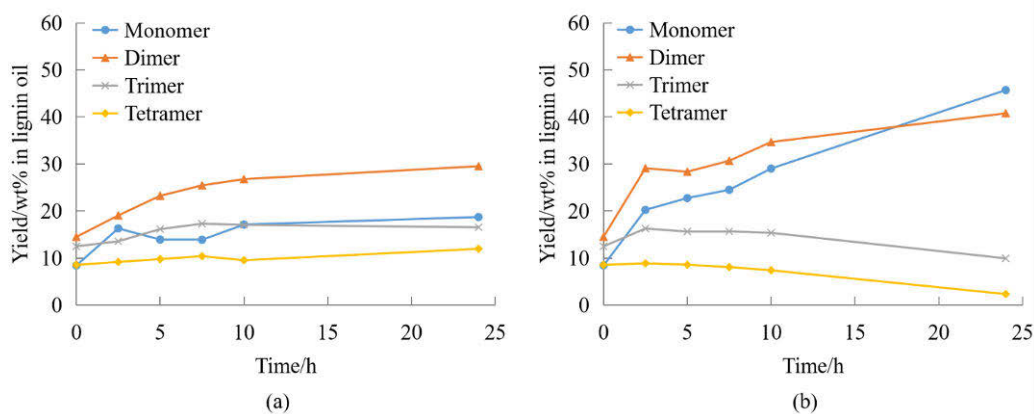


Figure 16. The yield of mono-, di-, tri-, and tetramer as a function of time for experiments performed in (a) EtOH-H₂O (50/50, v/v) and (b) MeOH-H₂O (30/70, v/v) mixtures catalyzed by 5% Ru/C under 20 bar H₂ and 240°C.

3.1.2.5 Effect of hydrogen pressure, temperature, and basic additives

Reaction parameters, such as temperature, pressure and pH can have a significant effect on the RCD process, as they not only influence the efficiency of depolymerization, but also the repolymerization and other side reactions, as well as the product distribution. Therefore, the influence of these parameters were investigated to gain a better understanding of the lignin depolymerization process.

As shown in Figure 17, there was only a small difference between the mono- to tetramer yield from experiments using different initial H₂ pressures, which implied that lower concentrations of H₂ employed in the reaction system were already sufficient to achieve similar hydrogenolysis and hydrogenation as at higher pressures. This would reveal that the catalyst surface was already covered with hydrogen at an initial pressure of 3 bar, and no additional benefit was brought to the lignin products by increasing the pressure. However, the use of higher hydrogen pressures practically helped raise the boiling point of the reaction mixture, preventing the loss of the possible volatile products.

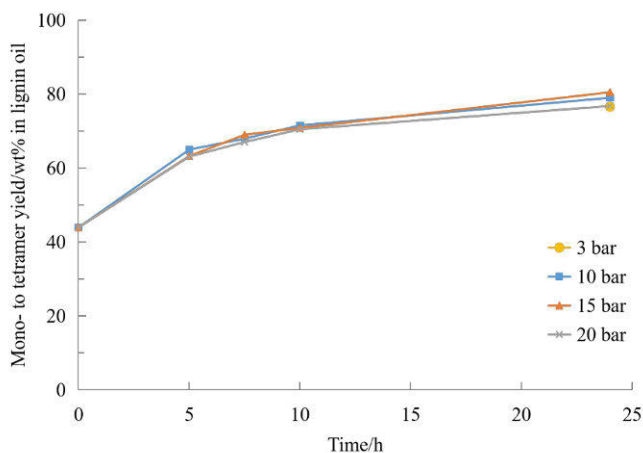


Figure 17. Effect of initial hydrogen pressure on the mono- to tetramer yield of the experiment in EtOH-H₂O (50/50, v/v) mixture catalyzed by 5% Ru/C at 240°C.

The samples obtained from experiments performed in EtOH-H₂O (50/50, v/v) mixture at different temperatures were analyzed by various methods. Intermediate samples were taken during the experiments performed at 210°C and 240°C whereas only the final liquid products were collected at 180°C due to the difficulty in sampling at lower pressure. It was evident from the HPSEC results, that an elevated temperature, at least 210°C, was required to achieve efficient conversion of lignin, since the mono- to tetramer yield at 180°C was only about 60% (Figure 18). However, a smaller difference was observed between the kinetics of reactions at 210°C and 240°C, although the reaction rates at 240°C was obviously higher than that at 210°C. Somewhat more monomers to tetramers (77% compared to 73%), as well as a slightly reduced polymeric fraction, were observed after 24 hours experiment at 240°C compared to 210°C. A decrease in the M_w of lignin oil products from 834 g/mol to 677 g/mol and further to 595 g/mol was observed when heating up the reaction mixture. Moreover, GC-FID/TCD results indicated that somewhat more gaseous products were formed at higher temperatures, and the content of CO₂, CO, C₃H₈ and C₄H₁₀ increased. 240°C was chosen for further experiments as a compromise between the selectivity and the kinetics.

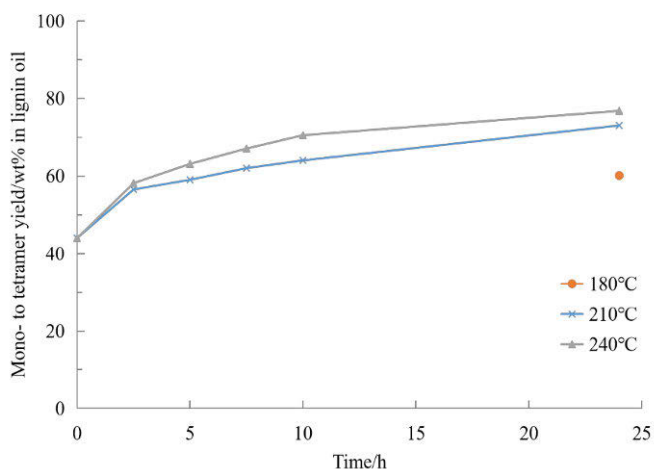


Figure 18. Effect of temperature on the mono- to tetramer yield of the experiment in EtOH-H₂O (50/50, v/v) mixture catalyzed by 5% Ru/C under 20 bar H₂.

Adding base has been proven to positively influence the RCD processes in previous studies [37]. Figure 19 compared the samples from two experiments with different amounts of NaOH added to the sample from a standard RCD experiment conducted under otherwise identical conditions. It is clear that more reactive bonds were cleaved faster in the beginning. Then the cleavage to mono- to tetramer slowed down. There were still certain bonds left in the material that cannot be cleaved with the developed methodology, which explains why 100% yield was not obtained. It can be concluded that adding NaOH slightly increased the yield of smaller aromatics, whereas it had a slightly more significant influence on polymer production. It also promoted the kinetics at the early stages of the experiment. However, the benefit of employing basic additives was concluded not to outweigh the problems caused by the salts in subsequent separation process.

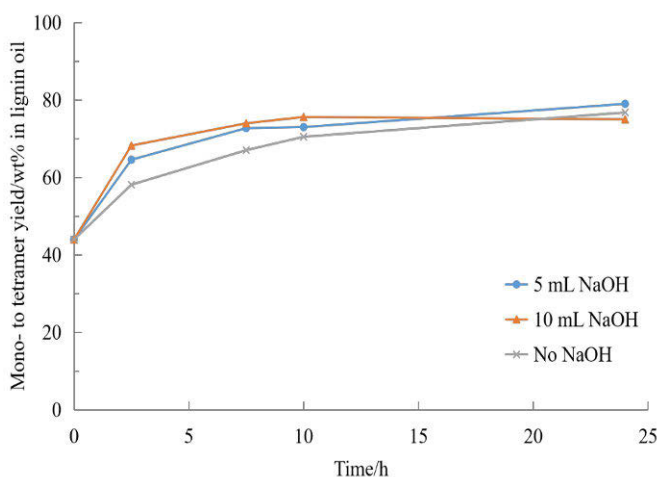


Figure 19. Effect of NaOH on the mono- to tetramer yield of the experiment in EtOH-H₂O (50/50, v/v) mixture catalyzed by 5% Ru/C under 20 bar H₂ and 240°C.

3.1.2.6 Effect of catalyst to substrate ratio

Catalysts are essential for chemical reactions, especially in large-scale production, to accelerate the acquisition of high yields of target products while suppressing unwanted reactions. Not only the type, but the loading of the catalyst is also very important, because it directly influences the concentration of active sites on the catalyst, where the chemical reactions take place.

Therefore, the influence of the catalyst amount was investigated by decreasing the loading. An equivalent of 0.27 g, 0.53 g, and 0.8 g 5% Ru/C catalyst (dry) was tested while keeping the lignin amount constant at 1 g. Other reaction parameters were kept identical. The results were shown in Figure 20, where the final mono- to tetramer yield decreased from 77% to 70% when the catalyst loading was decreased threefold. The difference was especially significant when only 0.27 g Ru/C was used; nevertheless, the dependence of the kinetics on the catalyst amount cannot be simply described as linear. The concentration of available sites on the catalyst can be assumed to be more than enough compared to the amount of lignin macromolecules with 0.8 g Ru/C. When the reaction proceeded and more moles of oligomers are formed in the reaction mixture, a difference can be observed between 0.8 and 0.53 g, as the concentration of available sites starts limiting the observed reaction rate. A significant decrease in kinetics when using 0.27 g catalyst was observed since the

beginning of the experiment, while the difference in the efficiency between 0.53 g and 0.8 g started to be visible first after 10 hours of experiment.

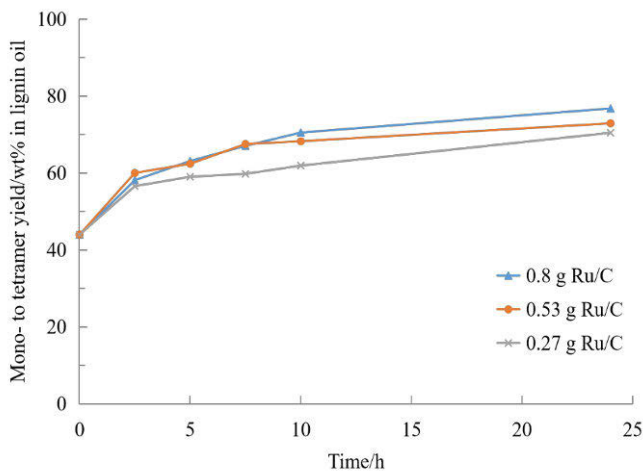


Figure 20. Effect of catalyst loading on the mono- to tetramer yield of the experiment in EtOH-H₂O (50/50, v/v) mixture catalyzed by 5% Ru/C under 20 bar H₂ and 240°C.

The amounts of lignin and catalyst (5% Ru/C) were doubled so that the catalyst/substrate ratio was maintained. The distribution of mono- and dimers did not differ significantly and the kinetics to produce desired lignin products with specific molar masses lower than tetramer were practically identical. This also confirmed that the solubility did not limit the depolymerization rate.

3.1.2.7 Effect of solvent and thermal degradation

The effect of water in the reaction medium was studied by conducting experiments in ethanol-water solution mixed at different volume ratios (30/70, 50/50), as shown in Figure 21(a). By comparing the results of intermediate samples, it was evident that an increase in the water content promoted the depolymerization kinetics. However, the weaker solubility of lignin in water prevented the use of very high water concentrations. Experiments conducted in EtOH-H₂O mixtures of volume ratios 30/70 and 50/50 produced 83% and 77% of mono- to tetramers, respectively. The higher polarity of the reaction medium caused by increased water proportion in

the mixture seemed to be beneficial to the RCD process by enhancing the fragmentation of the lignin oligomers to produce monomers and dimers [38].

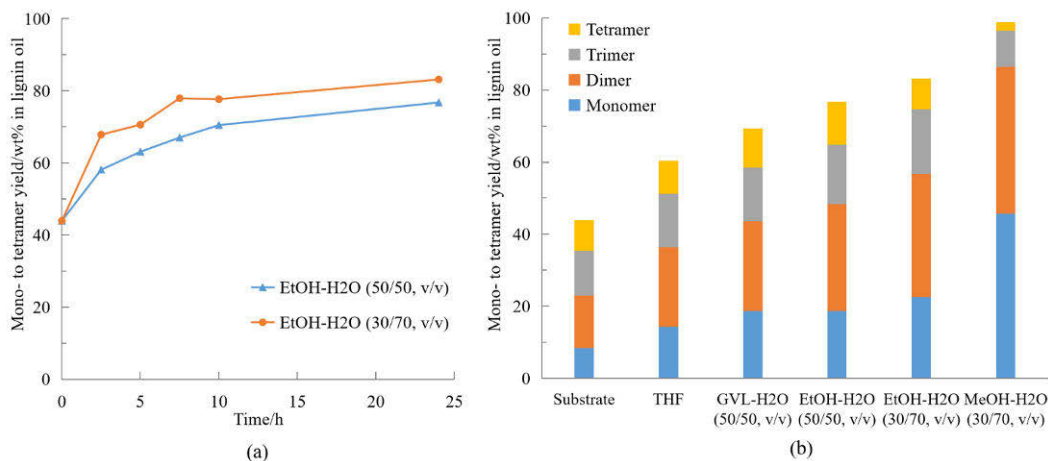


Figure 21. Effect of (a) ethanol-water ratio and (b) solvent type on the mono- to tetramer yield during and after a 24 hours experiment catalyzed by 5% Ru/C under 20 bar H₂ and 240°C.

The influence of the solvent type on the RCD process was also studied (Figure 21(b)). The order of decreasing M_w was concluded to be THF → GVL-H₂O (50/50, v/v) → EtOH-H₂O (all ratios) → MeOH-H₂O (30/70, v/v), which was consistent with the order of increase in the mono- to tetramer yield. Experiments conducted in THF produced 60% of lignin mono- to tetramers, while MeOH-H₂O (30/70, v/v) led to the highest yield (98%). The excellent performance of MeOH-H₂O mixture was attributed to its higher polarity and the ability of MeOH to prevent condensation due to its smaller molecular volume and greater hydrogen bonding ability [39]. MeOH most probably also acted as a hydrogen-donor [36], which favored the catalytic hydrogenolysis and hydrogenation processes. THF was proven to be the least efficient for depolymerization towards smaller aromatic compounds, in which the unstable lignin fragments were more likely to be repolymerized.

Two non-catalytic experiments were performed in MeOH-H₂O (30/70, v/v) and EtOH-H₂O (50/50, v/v) under argon atmosphere at 240°C to study the thermal degradation (Figure 22). It was demonstrated that lignin oil from the RCD process at 240°C was mainly a result of catalytic hydrogenolysis and hydrogenation, but that thermal degradation also played a role in the depolymerization partly depending on the solvent. ¹³C NMR analysis also confirmed this by

individual sharper peaks of the products than the substrate, indicating that the lignin macromolecules were cleaved into smaller compounds.

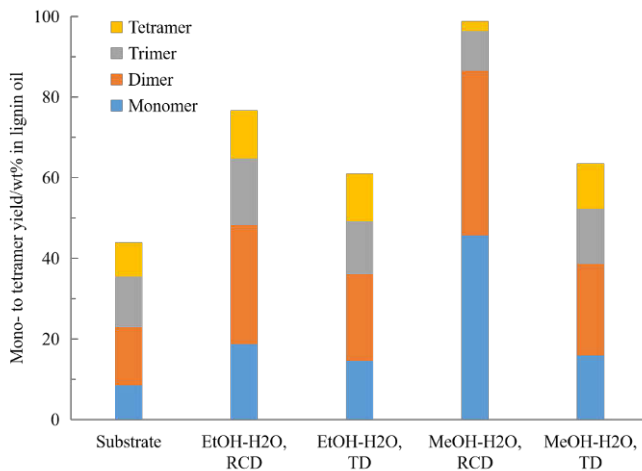


Figure 22. Comparison of the mono- to tetramer yield after 24 hours thermal degradation (TD) and standard RCD experiments at 240°C. RCD reaction employed 5% Ru/C and 20 bar H₂, while thermal degradation utilized 10 bar Ar without a catalyst.

3.1.3 Lignin oil mass balance

The mass balance of the RCD process was determined by performing experiments without taking intermediate samples. The yield of lignin oil was calculated by Equation 1. The results showed around 70% yield for standard RCD experiments and above 90% for non-catalytic experiments. The difference in the yield might be caused by char formation by random repolymerization of the active radicals [40] and/or gas formation by either decarbonylation/decarboxylation or cleavage of aliphatic side chains and ring substituents during the catalytic hydrotreatment [41].

It can be concluded from the GC-FID/TCD results that the main gaseous product from RCD experiments was methane produced by hydrogenolysis of Ph-OCH₃ groups, which accounted for around 85% of the gas mixture. Other gases formed involve ethane, propane, butane, and CO₂, which were also reported in the literature [41]. The composition of these minority gases varied according to the reaction conditions, especially to the solvent employed. Thermal degradation in

MeOH-H₂O (30/70, v/v) has produced a little more ethane and propane than other experiments, while some CO was also detected.

3.1.4 Structural characterization of raw material and reaction products by NMR

The samples obtained from the thermal degradation and RCD experiments in EtOH-H₂O (50/50, v/v) and MeOH-H₂O (30/70, v/v) were analyzed qualitatively by 2D HSQC NMR, ¹³C NMR and quantitatively by ³¹P NMR. The studied RCD experiment was catalyzed by Ru/C under 20 bar H₂, while no catalyst was used in the thermal degradation under 10 bar Ar. From the HSQC-spectrum of the starting material, the C-H correlation peaks from both syringyl- and guaiacyl units, enol ether and fatty acids could be detected in the aromatic region. In the oxygenated aliphatic area, the correlation peaks corresponding to signals from the –OMe groups, β-β substructure, carbohydrate impurities and the aryl glycerol end-group were detected. In the aliphatic region, the main correlation peaks were from fatty acid impurities. In all four processed samples, the identifiable correlation peaks, besides the –OMe group, were removed in the oxygenated aliphatic region. Considerable amounts of correlation peaks of CH₂ was observed below the –OMe correlation peak. These most likely originate from primary alcohols that can have formed from partially dehydroxylated side chains. In the aliphatic region, correlation peaks consisted of CH/CH₃ and CH₂ were detected in different clusters. The chemical shifts of these clusters are in agreement with previously published shifts of saturated aliphatic side chains (methyl, ethyl, propyl) and also partially dehydroxylated side chains [42,43]. The RCD samples had a slightly lower proton chemical shift in the aromatic region compared to the substrate and the thermal degradation samples. Correlation peaks at a higher proton shift in the aromatic region are often assigned as aryl rings with oxidized α-positions. A new cluster was detected in the thermally treated samples, which could originate from stilbene structures, α,β-unsaturated carbonyl structures, demethoxylated lignin units and some signals from oxidized G-units. As for the samples from RCD reactions, the significant reduction in these structures was most likely due to the reductive process. The incorporation of the solvent was evident from the methyl ester correlation peak in the samples that used MeOH-H₂O mixture and the correlation peak of the CH₂ in the samples corresponding to EtOH-H₂O mixture. The fragmentation of all these processed samples can be observed in ¹³C NMR according to the considerably sharper peaks compared to the substrate. The signal assigned to C-3/C-5 in etherified S units had almost completely been removed in the processed samples.

The amounts of free hydroxyl groups analyzed by ^{31}P NMR were listed in Table 5. The results indicated that the lignin polymers were cleaved into smaller compounds, when comparing to the substrate, by producing more free hydroxyl groups during the experiment. In addition, the amount of carboxyl group was shown to decrease via experiments, which can be explained by the decarboxylation to form gaseous products. The RCD experiment conducted in MeOH-H₂O mixture had significantly increased the amount of free aliphatic hydroxyl groups compared to other experiments.

Table 5. Amount of free hydroxyl groups in mmol/g based on ^{31}P NMR analysis.

	Aliphatic	S-units ^a	G-units ^b	Ph-OH	OH total	COOH
Substrate	1.32	2.31	0.77	3.08	4.40	0.66
MeOH-H ₂ O, RCD	1.83	2.92	1.60	4.52	6.35	0.48
EtOH-H ₂ O, RCD	1.00	2.77	1.14	3.91	4.91	0.41
MeOH-H ₂ O, thermal degradation	0.87	3.11	1.52	4.63	5.50	0.36
EtOH-H ₂ O, thermal degradation	0.90	2.87	1.24	4.11	5.01	0.34

^a S-units and/or condensed G-units

^b G-units and H-units

3.1.5 Identification of lignin oil products by GC-MS

The lignin oil products after a 24 hours RCD experiment in EtOH-H₂O (50/50, v/v) mixture catalyzed by 5% Ru/C under 20 bar H₂ and 240°C were also characterized by GC-MS, which was in agreement with NMR results. It can be concluded from the results that the most abundant monomers among all compounds detected were: syringol, 4-methylsyringol, 3,4-dimethoxy-5-hydroxysyringaldehyde, homosyringaldehyde, 2-guaiacylethanol, 2-syringylethanol, and 3-vanil-1,2-propanediol, as displayed in Figure 23. The results were also confirmed by GC-FID analysis. The structures of these most abundant monomer products indicated that the phenolic hydroxyl and methoxyl groups remained largely intact during the depolymerisation; however, the aliphatic region underwent cleavage of varying extent all the way to being completely removed in the case of syringol.

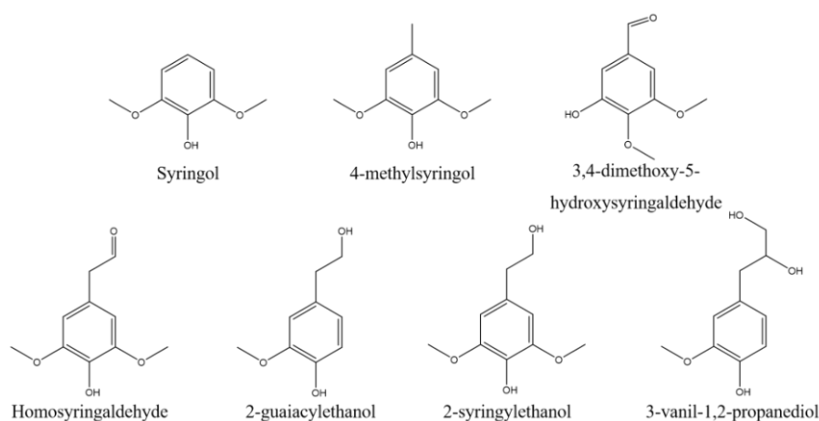


Figure 23. The most abundant monomer structures in the product mixture.

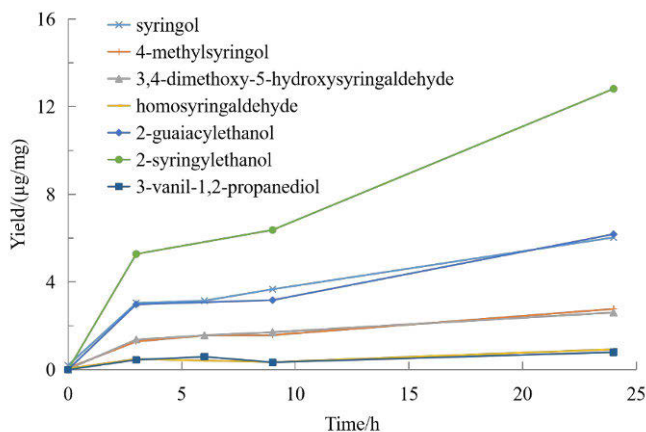


Figure 24. The yield of the most abundant monomers as a function of time for a non-catalytic experiment in EtOH-H₂O (50/50, v/v) mixture under 20 bar H₂ and 240°C characterized by GC.

The concentrations of the monomeric products mentioned above were determined for non-catalytic experiment in EtOH-H₂O (50/50, v/v) mixture (Figure 24) and catalytic experiments in EtOH-H₂O (50/50, v/v) and MeOH-H₂O (30/70, v/v) mixtures (Figure 25). The results clearly showed that the product distribution was different. 2-syringylethanol, 2-guaiacylethanol and syringol were the most abundant in the non-catalytic experiment, while 2-syringylethanol dominated. In the catalytic experiments, syringol was the most abundant one, indicating a severer cleavage of the aliphatic chains. In addition, the consecutive reaction pathway also observed previously with HPSEC (Figure 16) was evident especially when methanol-water mixture was

employed, since the monomer concentration increased significantly first after 10 hours of experiment. On the other hand, clearly certain bonds were cleaved easier and faster than others, which explains the slow down in the reaction rates as the experiments proceeded. ^{31}P NMR results also indicated that more free hydroxyl groups were produced during the experiment, i.e., certain bonds, such as $\beta\text{-O-4}$ and $\alpha\text{-O-4}$, were cleaved. As the reaction proceeding, the concentration of these bonds decreased, which led to a lower accessibility of the bonds to the active sites of the catalyst and finally resulted in slower reactions.

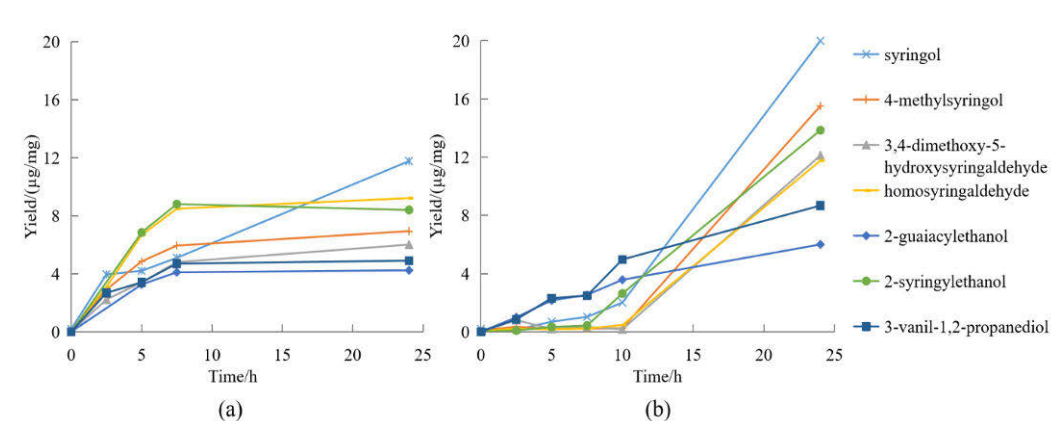


Figure 25. The yield of the most abundant monomers as a function of time in (a) EtOH-H₂O (50/50, v/v) and (b) MeOH-H₂O (30/70, v/v) mixtures catalyzed by 5% Ru/C under 20 bar H₂ and 240°C characterized by GC.

3.1.6 Characterization of different fractions from ultra-filtration

The lignin oil product after a 24 hours experiment in EtOH-H₂O (50/50, v/v) mixture under 20 bar H₂ and 240°C were introduced to ultra-filtration. The filtrate was gathered, dried and characterized with GC-FID, HPSEC, and different NMR methods.

Structurally the filtrate was similar to the lignin oil product before ultra-filtration according to 2D HSQC and ^{13}C NMR. However, the filtrate contained higher amounts of hydroxyl groups, which was indicated by sharper peaks in the ^{31}P NMR spectra. The concentration of hydroxyl groups was found to increase from 4.91 mmol/g to 6.44 mmol/g after ultra-filtration. Moreover, the M_w of filtrate was calculated to be 434 g/mol with HPSEC, corresponding to DP of around 3.

Quantitative GC results showed that the concentration of identified monomers and dimers nearly doubled after ultra-filtration.

The residue of ultra-filtration was involved in a further oxidation process. The samples before and after the oxidation experiment were analyzed with HPSEC. The results indicated that the large molecule fractions obtained from the RCD process cannot be further degraded efficiently, at least via oxidation. The M_w value was only slightly decreased from 1590 g/mol to 1292 g/mol.

3.2 Catalytic hydrolysis of semi-industrial hemicellulose to monosaccharides in batch reactor

Part of this chapter is adapted from the post print of the following article:

X. Lu, P. Junghans, J. Wärnå, G. Hilpmann, R. Lange, H. Trajano, K. Eränen, L. Estel, S. Leveneur, H. Grénman. Hydrolysis of semi-industrial aqueous extracted xylan from birch (*betula pendula*) employing commercial catalysts – kinetics and modelling. *Journal of Chemical Technology & Biotechnology*, doi: 10.1002/jctb.6918.

Link: <https://doi.org/10.1002/jctb.6918>

Further permissions related to the material excerpted should be directed to the Wiley. Copyright © 2021 John Wiley & Sons, Inc.

Xylose is a very useful functional monosaccharide derived from hemicellulose, which is used in the production of chemicals, hydrogen, veterinary supplies and many other products. Acid hydrolysis is a conventional method of converting xylan to produce xylose. In this chapter, the acidic hydrolysis process was studied in a batch reactor. Hemicellulose produced by a novel semi-industrial process was selected as the raw material. Several commercial heterogeneous catalysts were screened and the kinetics were studied under varying experimental conditions. The goal was to achieve the highest xylose yield and as few dehydration products as possible. A mathematical model was also developed to describe the reaction kinetics. Some of the experiments were repeated three times and the relative standard deviation was determined to be within 1.5-8.8%.

3.2.1 Catalyst screening

Five different acidic heterogeneous catalysts were selected for catalyst screening [44]. Based on literature and preliminary results obtained at ambient pressure, relatively high temperature and low pH are required in the hydrolysis of xylan compared to e.g. inulin [44,45]. 115°C was selected as the operating temperature in the screening considering the maximum operating temperatures of the catalysts. A pH of 0.75 was used to maintain a reasonable solid-liquid ratio. The experiments were performed with a total volume of 200 mL for 8 h under isothermal conditions and the results are shown in Figure 26.

The xylose yield increased rather linearly with Amberlite IR120, Dowex 50WX8-50, and Amberlyst 15. Amberlite IR120 and Dowex 50WX8-50 resulted in the least efficient conversion with a xylose yield of 40% after 8 hours while with Amberlyst 15 60% was obtained. The reaction rate was significantly faster with Dowex 50WX2-100 and Smopex 101 and a xylose yield of over 60% was obtained in less than 4 hours, after which the yield was rather stable. The big difference between the performances of the two Dowex catalysts demonstrated that the pore size, which is closely related to the degree of crosslinking, significantly influenced the catalytic results. That is because more crosslinking results in smaller pores and the bulky xylan molecules are more sterically hindered from diffusing inside the catalyst particles. Dowex 50WX2-100 was selected for further experiments considering its stronger ion exchange capacity and higher maximum operating temperature (150°C). Moreover, the experimental results were successfully reproduced with recycled catalyst for at least 3 times.

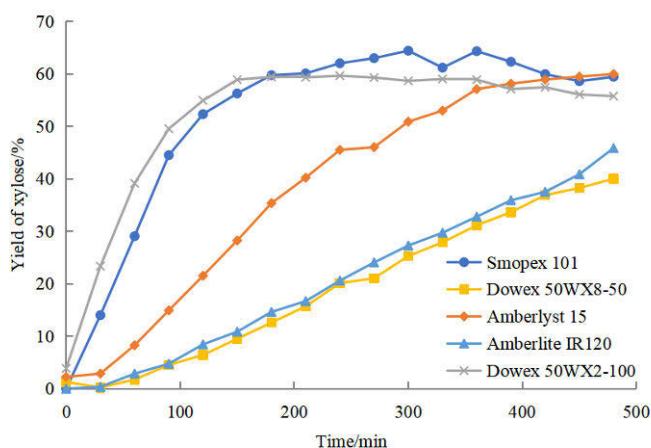


Figure 26. Influence of catalyst on the yield of xylose in experiments performed at 115°C and pH 0.75.

3.2.2 Influence of stirring speed

Different stirring speeds were tested under identical conditions to see if the agitation was intense enough to eliminate the influence of external mass transfer limitations. 137°C and pH 0.75 were selected to ensure the necessary reaction rate to make the influence of external mass transfer visible.

A significant difference in the reaction rate corresponding to 320 rpm and 660 rpm were observed in Figure 27. The observed kinetics for both hydrolysis and consecutive side reaction (i.e., dehydration of xylose) were much slower at a lower agitation rate. The difference between the kinetics at 660 rpm and 850 rpm was practically negligible and it could be concluded that 660 rpm provided sufficient turbulence.

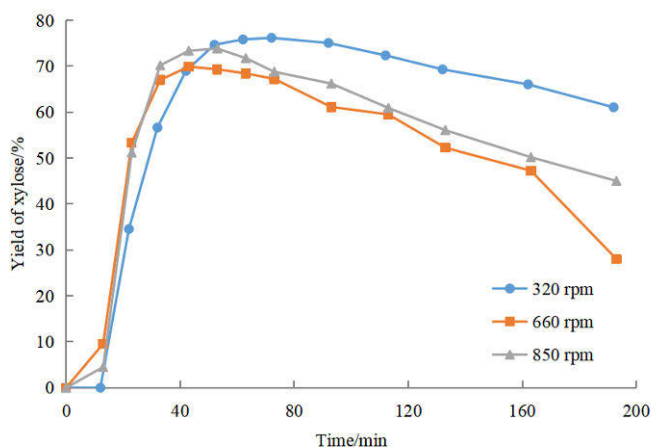


Figure 27. Influence of stirring speed on the yield of xylose in experiments performed at 137°C and pH 0.75 with Dowex 50WX2-100.

3.2.3 Influence of pH

The influence of pH was also investigated under otherwise identical conditions. A temperature of 145°C was chosen to ensure that severe degradation could take place. Four different pH values were chosen between 0.5 to 1.5, giving a tenfold variation in the concentration of protons. It is evident in Figure 28 that the kinetics of the hydrolysis was heavily influenced by pH, whereas the dehydration rate also increased with lower pH, which was evidenced by a rapid decline in xylose concentration as soon as the highest yield was reached. Naturally, the influence on the kinetics already commenced at the beginning of the experiments. As a consequence, only a very small amount of xylose was remaining after 3 hours of experiment. Nevertheless, pH 0.5 gave the highest xylose yield (71%) and the experiment at pH 1 did not yield as much xylose as at lower pH, but the hydrolysis was clearly faster than at pH 1.5 and the xylose concentration was relatively stable for 30 min. In the experiment at pH 1.5, it took about 70 min to reach the highest xylose yield.

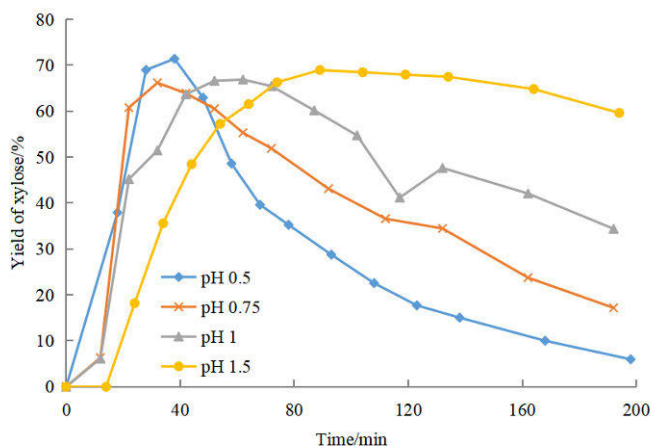


Figure 28. Influence of pH on the yield of xylose of experiments performed at 145°C with Dowex 50WX2-100.

3.2.4 Influence of temperature

The influence of temperature on the kinetic was studied at a pH of 0.75 as pH 0.5 was already very harsh and led to rapid dehydration. Three temperatures (130°C, 137°C and 145°C) were selected for evaluating its influence on both the hydrolysis and dehydration kinetics. The results were shown in Figure 29.

The kinetics at higher temperature was considerably faster. The highest xylose yield (66%) was achieved in only 20 min at 145°C, whereas at 115°C it took 3 hours to reach the same yield. However, the highest yield obtained at 145°C was lower than those at lower temperatures. Significant dehydration has taken place immediately after the maximum was reached, and a xylose yield of only 17% was obtained after 3 hours experiment. The hydrolysis kinetics at 137°C was slightly slower than that at 145°C, but a higher xylose yield (70%) was reached and no degradation was observed for the first 40 min even though some degradation most probably occurred. There was about 28% xylose left after 3 hours experiment. The kinetics at 130°C was even slower and 72% xylose was obtained after 40 min. However, the degradation was slow and the dehydration started to be visible after about 50 min, resulting in a relatively high xylose yield (60%) in the end. It was evident that the kinetics are very temperature sensitive and careful optimization is required when performing the reaction in, e.g., a larger batch reactor or a continuous reactor.

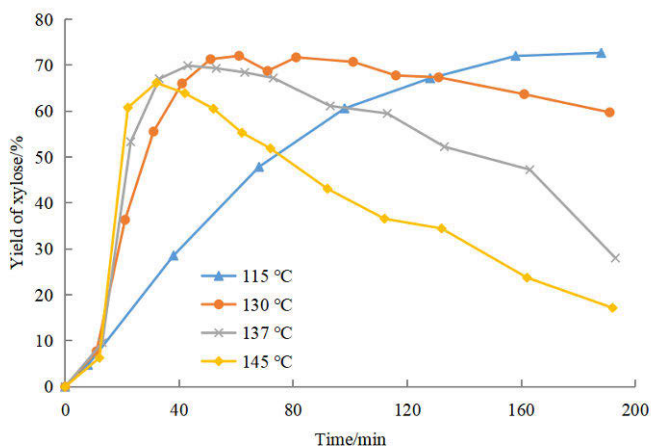


Figure 29. Influence of temperature on the yield of xylose in experiments performed at pH 0.75 with Dowex 50WX2-100.

3.2.5 Influence of particle size of the catalyst

The Dowex 50WX2-100 (50–100 mesh) catalyst employed in the previous experiments has a particle size between 300 and 150 μm . Another Dowex catalyst with a smaller particle size of 200 to 400 mesh (37–75 μm) was also tested at 137°C and pH 0.75 in order to observe the influence of internal mass transfer resistance on the kinetics.

Figure 30 indicated that the catalyst with smaller particle size was slightly more efficient. The highest xylose yield of 74% was obtained in 30 min after reaching the desired temperature. Two-fifths of the produced xylose were then degraded, leading to a final xylose yield of 47% after 3 hours experiment. The kinetics with Dowex 50WX2-100 was slower, while the highest yield was achieved in 60 min and less dehydration was observed. The xylose yield decreased to 61% in the end. It can be concluded that both the hydrolysis and dehydration were faster when smaller catalyst particles were employed. This was probably due to the larger external surface area of the smaller catalyst particles and the decrease in the internal mass transfer limitations. However, the difference observed in the kinetics was not significant when considering performing hydrolysis in e.g. a continuous reactor.

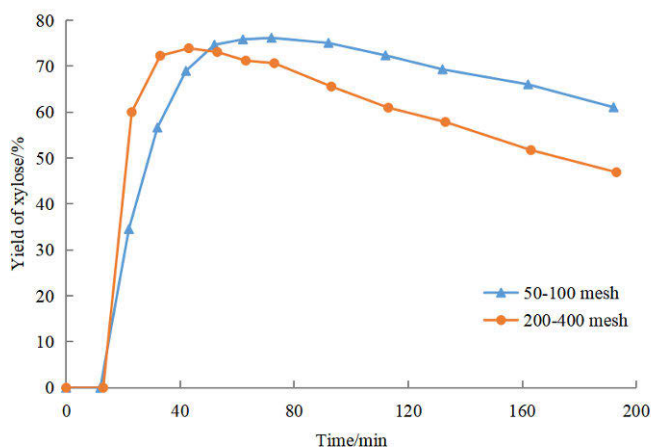


Figure 30. Influence of catalyst particle size on the yield of xylose of experiments performed at 137°C and pH 0.75 with Dowex 50WX2 catalysts.

3.2.6 Catalyst stability

A preliminary catalyst deactivation study was carried out at a temperature of 137°C and a pH of 0.2, with a high xylan concentration of 20g/L. Catalyst stability started to decrease significantly after about 34 hours due to the pore blockage, which is most probably caused by the repolymerization of degradation products [46,47]. This indicates that process optimization avoiding degradation of monosaccharides is extremely important also for the catalyst stability. This ties the sugar degradation study closely to studying the deactivation of the catalyst employed for hydrolysis.

3.2.7 Mathematical modelling

A mathematical model was developed based on the batch reactor data to quantify the influence of different experimental parameters on the kinetics. Preliminary experimental and literature data suggested that the hydrolysis of xylan proceeded through a type of “end-biting” mechanism, in which monomers and short oligomers are cleaved from the end of the macromolecules. During the experiment, the long xylan polymeric chain were cleaved into smaller molecules, producing more bonds that were easily accessible, which leads to an increase probability of an encounter of the protons in the sulfonic groups of the catalyst and the glycosidic bonds and finally results in a greater

reaction rate, i.e., observed autocatalysis. The small xylooligomers detected with HPLC confirmed this hypothesis.

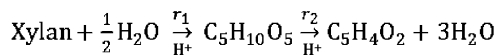
A recently developed two-parameter model that takes the autocatalytic effect into account [44] was utilized.

$$k = k_0(1 + \beta X^\alpha) \quad (17)$$

$$\beta = \frac{(k_\infty - k_0)}{k_0} \quad (18)$$

where k is the conversion dependent observed rate constant, k_0 is the reaction rate constant, X is the conversion of xylan, α and β are constants.

The overall reaction can be described by a two-step consecutive reaction pathway



The reactions were considered irreversible and first order with respect to the reactants and the proton concentration according to the reaction mechanism and the concentration of water was assumed to be abundant and constant, so it was excluded from the model. Hence the reaction rates are described as follows:

$$r_1 = k_1 c_H + c_{xylan} \quad (19)$$

$$r_2 = k_2 c_H + c_{xylose} \quad (20)$$

A modified form of the Arrhenius equation was used to decouple the correlation of the pre-exponential factor and the activation energy.

$$k_0 = k_{01} \exp\left(-\frac{E_a}{R\theta}\right) \quad (21)$$

$$\frac{1}{\theta} = \frac{1}{T} - \frac{1}{T_{ref}} \quad (22)$$

where k_{01} is the pre-exponential factor, E_a the activation energy, R the universal gas constant, and θ the modified temperature. The reference temperature T_{ref} was 137°C.

The mass balance for each compound in the reaction mixture employing a modified Arrhenius equation was then expressed as:

$$\frac{dc_{xyylan}}{dt} = -k_{01} \exp\left(-\frac{E_{a1}}{R\theta}\right) \left(1 + \beta \left(\frac{c_{xylose}}{c_{xylose}^0}\right)^\alpha\right) c_{H^+} c_{xyylan} \quad (23)$$

$$\frac{dc_{xylose}}{dt} = \left(k_{01} \exp\left(-\frac{E_{a1}}{R\theta}\right) \left(1 + \beta \left(\frac{c_{xylose}}{c_{xylose}^0}\right)^\alpha\right) c_{H^+} c_{xyylan}\right) - k_{02} \exp\left(-\frac{E_{a2}}{R\theta}\right) c_{H^+} c_{xylose} \quad (24)$$

$$\frac{dc_{degr.}}{dt} = k_{02} \exp\left(-\frac{E_{a2}}{R\theta}\right) c_{H^+} c_{xylose} \quad (25)$$

c_{H^+} denoted the concentration of the protons that can be calculated based on the number of sulfonic acid sites in the catalyst.

For the kinetic parameter estimation, a non-linear regression analysis that included parts of the experimental data was utilized. The data of xylose concentration was emphasized in the modelling as the xylan concentration measurement was slightly influenced by minor amounts (2.7% of total) of sulfonic groups leached from the catalyst. Moreover, xylan probably also underwent some repolymerization with the degradation products at the end of the experiment.

The model consisting of a system of ordinary differential equations (ODEs) was solved with the backward difference method implemented in the MODEST software. The sum of residual squares Q was calculated according to:

$$Q = \|c_{exp} - c_{est}\|^2 \quad (26)$$

The objective function Q was then minimized by the Simplex-Levenberg-Marquard method, where c_{exp} represents the concentration obtained in the experiment and c_{est} the concentration calculated by the model.

The value for α was very close to unity, which implied that the correlation of the rate constant and the xylan conversion was linear. In addition, the value for β was practically 0, which suggests that no autocatalysis occurred or the autocatalytic effect was covered by the degradation of sugar products, especially in harsher conditions. Therefore, the model was simplified to:

$$\frac{dc_{xyylan}}{dt} = -k_{01} \exp\left(-\frac{E_{a1}}{R\theta}\right) c_{H^+} c_{xyylan} \quad (27)$$

$$\frac{dc_{xylose}}{dt} = k_{01} \exp\left(-\frac{E_{a1}}{R\theta}\right) c_H + c_{xylan} - k_{02} \exp\left(-\frac{E_{a2}}{R\theta}\right) c_H + c_{xylose} \quad (28)$$

$$\frac{dc_{degr.}}{dt} = k_{02} \exp\left(-\frac{E_{a2}}{R\theta}\right) c_H + c_{xylose} \quad (29)$$

A good fit of the model to the experimental data was obtained ($R^2=97.59$), as shown in Figures 31 and 32. The parameter values are listed in Table 6.

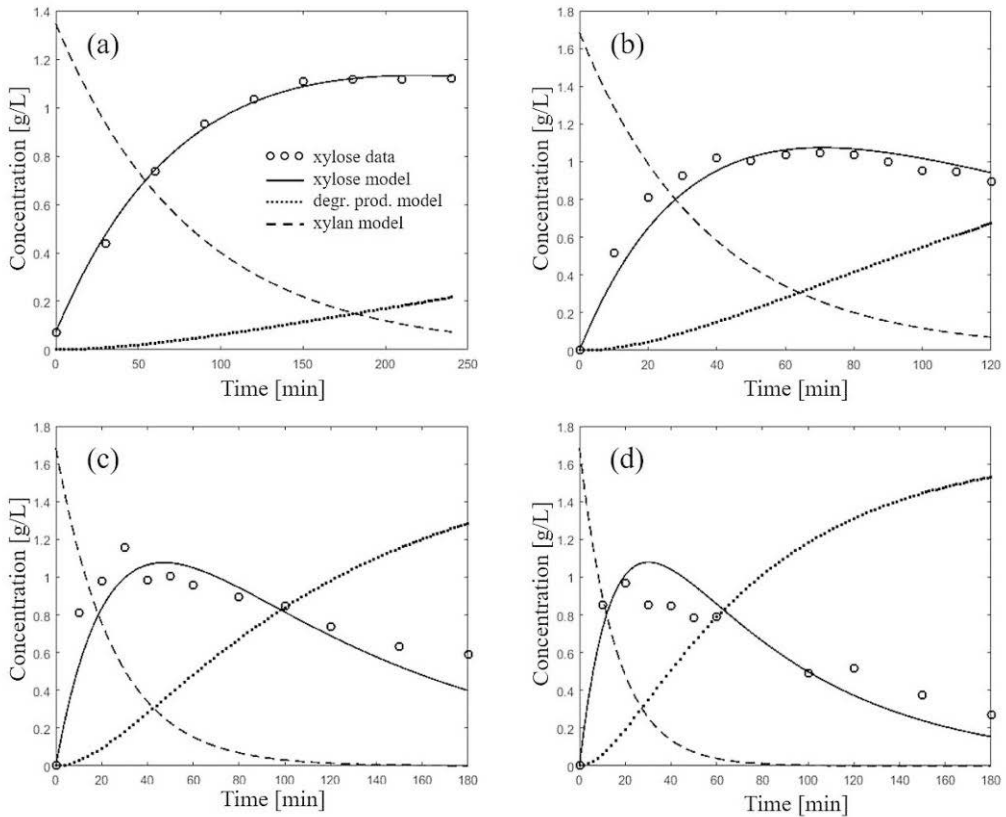


Figure 31. The concentrations of the xylan, xylose and degradation products as a function of time in experiments performed at pH 0.75 and different temperatures: (a) 115°C, (b) 130°C, (c) 137°C and (d) 145°C. The lines represent the model prediction and the circles represent the experimental xylose concentration.

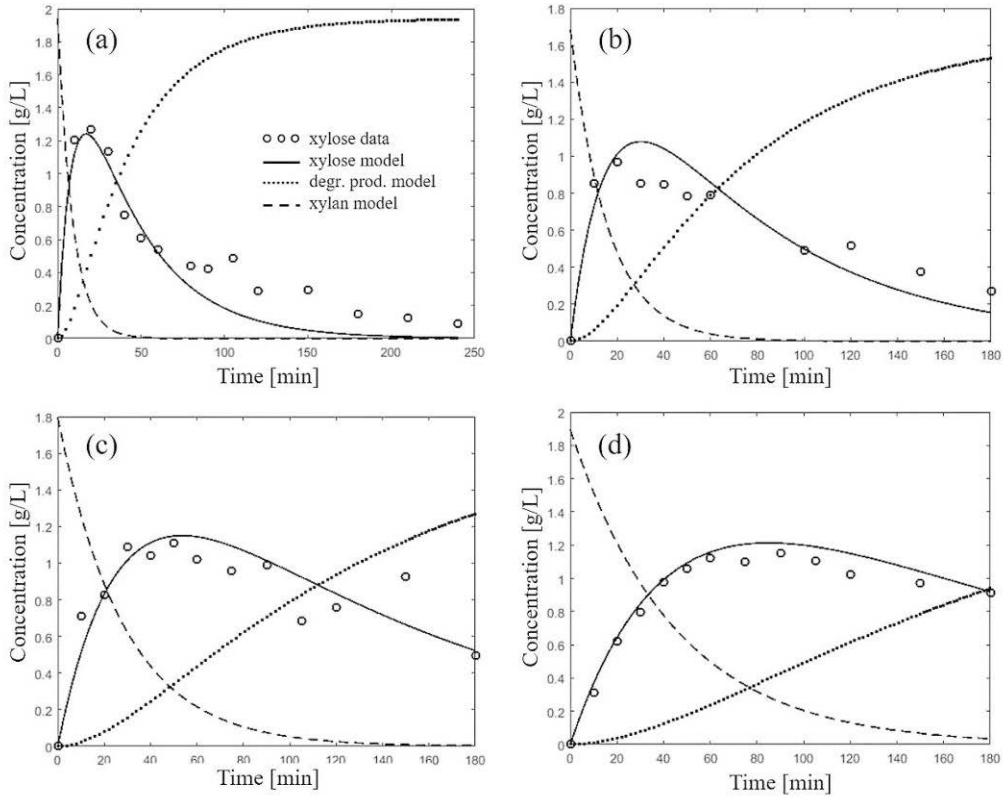


Figure 32. The concentration of xylan, xylose and degradation products as a function of time in experiments performed at 145°C and different pH: (a) pH 0.5, (b) pH 0.75, (c) pH 1 and (d) pH 1.5. The lines represent the model prediction and the circles represent the experimental xylose concentration.

Table 6. Parameters after the final modelling approach.

Parameter	Value		Est. relative standard error %
k_1	0.149	L	5.0
k_2	0.0357	$\frac{\text{mol}}{\text{mol} \cdot \text{min}}$	6.2
E_{a1}	80300	kJ	6.6
E_{a2}	78900	$\frac{\text{kJ}}{\text{mol}}$	8.3

A sensitivity analysis was carried out on the obtained parameters. The contour plots (Figure 33) indicated that the correlation of the parameters was low and that they were well defined.

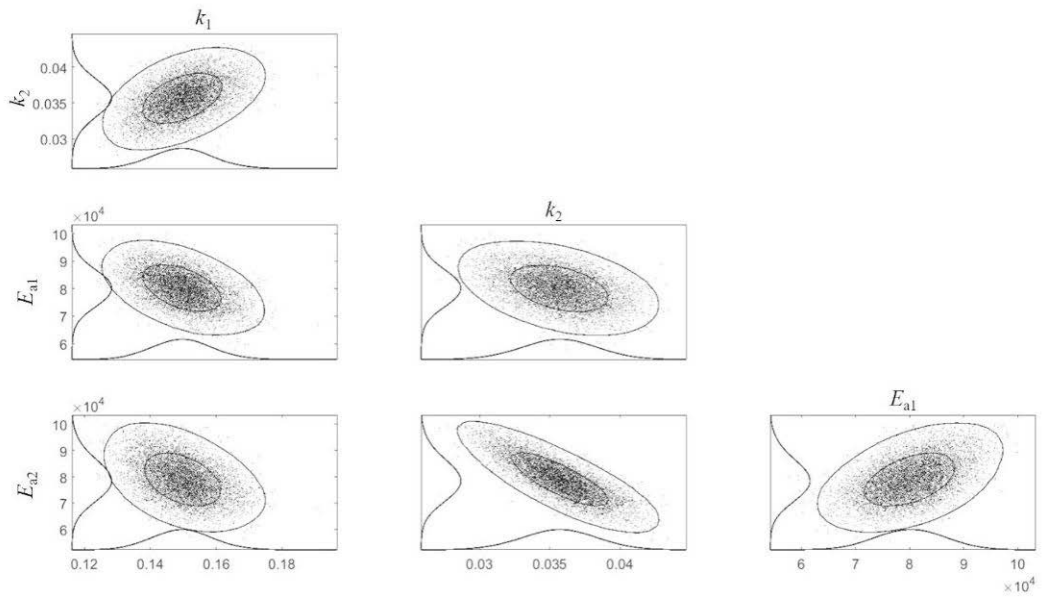


Figure 33. Contour plots of the correlation of the parameters.

3.3 Catalytic hydrolysis of semi-industrial hemicellulose to monosaccharides in continuous reactor

Part of this chapter is adapted from the post print of the following article:

X. Lu, P. Junghans, S. Weckesser, J. Wärnå, G. Hilpmann, R. Lange, H. Trajano, K. Eränen, L. Estel, S. Leveneur, H. Grénman. One flow through hydrolysis and hydrogenation of semi-industrial xylan from birch (*betula pendula*) in a continuous reactor – kinetics and modelling. *Chemical Engineering and Processing - Process Intensification*, 2021, **169**, 108614.

Link: <https://doi.org/10.1016/j.cep.2021.108614>

Further permissions related to the material excerpted should be directed to the Elsevier. Copyright © 2021 Elsevier B.V. or its licensors or contributors.

Based on the results of batch experiments, a continuous reactor system was designed and constructed in order to study the viability of a continuous process to achieve efficient conversion of the novel semi-industrial xylan. Dowex 50WX2-100 was used based on the catalyst screening result obtained in batch reactor. Moreover, the catalyst was observed to be very stable under the investigated conditions as only 2.7% of sulfonic groups were observed to be leached from the catalyst in stability tests. A low xylan concentration (2g/L) was used in most experiments, whereas a few were also carried out using a higher concentration (20g/L) to study the influence of the concentration. However, no significant difference was observed. This is most probably due to that the catalyst influences the local pH in close vicinity of the catalyst and, thus, acts as a “pseudohomogeneous” catalyst. The lower xylan concentration was mainly employed considering the experimental and analytical convenience. The reaction conditions (temperature, pH and residence time) were optimized to make a compromise between the kinetics of acidic hydrolysis and the undesired degradation of monosaccharide products. Moreover, a mathematical model was proposed, and good fit was obtained between the model and experimental data. Some of the experiments were repeated three times and the relative standard deviation was determined to be typically below 3.1%.

3.3.1 Influence of pH

The influence of pH on the reaction kinetics at 137°C and 145°C is shown in Figure 34. It was demonstrated that pH has a clear influence on the reaction kinetics. It can be concluded that at lower residence times, lower pH resulted in higher xylose yields as the kinetics of hydrolysis was promoted. On the other hand, at longer residence times, the yield of xylose decreased with increasing kinetics when lower pH was employed, as the consecutive dehydration of the monosaccharides increased. At a higher pH, however, the concentration of xylose gradually increased with the prolongation of retention time while little degradation was observed. It seems logical that a close to linear dependence of the xylose concentration (yield) as a function of residence time was obtained under investigated conditions before severe degradation started to take place. This is consistent with the batch reactor results, even though the dehydration at higher residence times did not lead to equally advanced dehydration as in the batch reactor at corresponding experimental time. Moreover, by simply comparing the experimental data shown in the two figures, a preliminary conclusion can be drawn that higher temperature promotes the reaction kinetics, whereas the side reaction is also accelerated. The degradation of sugar products can be clearly observed at shorter retention times, already at 20 min, when 145°C was employed.

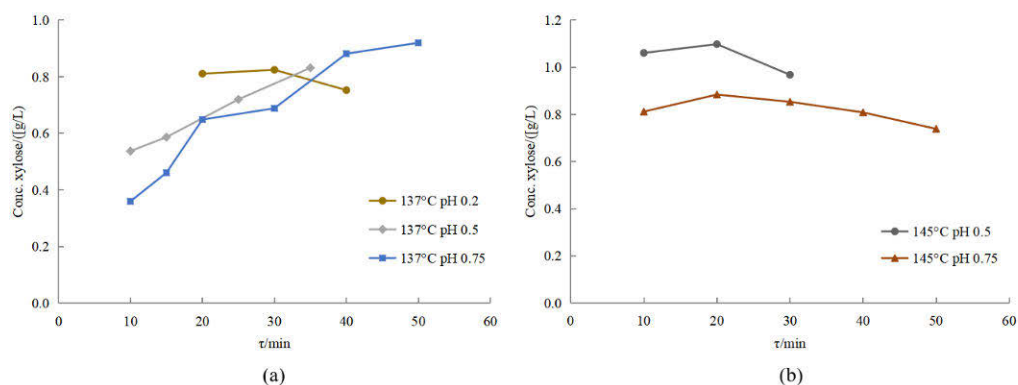


Figure 34. The xylose concentration as a function of residence time for experiments performed at (a) 137°C; (b) 145°C and different pH.

3.3.2 Influence of temperature

The effect of temperature on the kinetics of hydrolysis at pH 0.75 and 0.5 was displayed in Figure 35. The results indicated that at lower residence times, the yield of xylose increased with higher

hydrolysis reaction rate caused by elevated reaction temperature. When higher mean residence times were employed, the dehydration of monosaccharide products increased more significantly and higher yields were observed at lower temperature and a constant pH of 0.75. A similar trend was observed at pH 0.5. This is also in compliance with the results of previously performed batch experiments, however, the undesired degradation of xylose was not as profound at corresponding residence time compared to batch reactor experiment at the same experimental time. Moreover, a significant difference in the reaction rate was observed by heating the reaction mixture by 8°C, from 137 to 145°C, which clearly demonstrated a high activation energy of the reactions involved. Given this, it is evident that optimization of the reaction temperature is very crucial to the acidic hydrolysis process. A general conclusion can be drawn that high yields of monosaccharides can be achieved at high temperature and low pH, however, the retention time has to be kept very short in order to avoid degradation of desired sugar products.

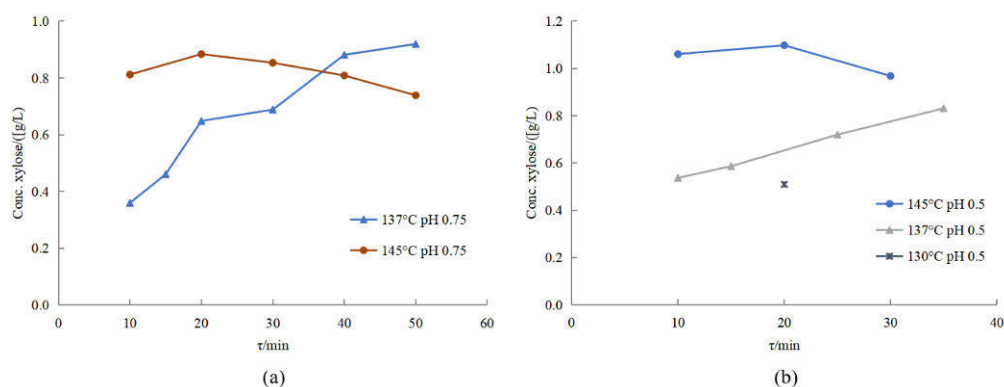


Figure 35. The xylose concentration as a function of residence time for experiments performed at (a) pH 0.75; (b) pH 0.5 and different temperatures.

Figure 36 displayed the mass distribution of compounds determined in the products at three different temperatures and a low pH of 0.3. The results demonstrated that when the temperature exceeded 140°C, the amount of degradation products as well as some condensation products that were detected as xylooligomers increased significantly. At 145°C, the degradation of monosaccharides was already severe.

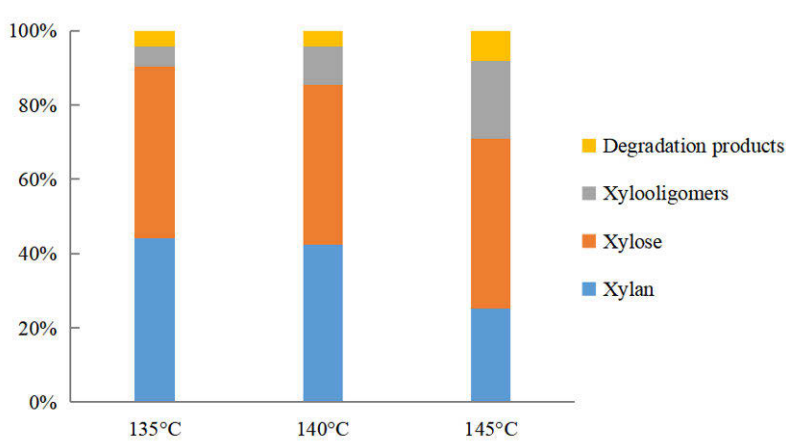


Figure 36. Influence of temperature on the mass distribution of products for experiments performed at pH 0.3 and a residence time of 12.3 min.

3.3.3 Influence of local pH

The influence of local pH was studied by evenly distributing 3.6 g of catalyst to achieve local pH of 0.3 and 0.5 and performing experiments at 135–145°C. The results were shown in Figure 37, where the xylan conversion were generally higher at pH 0.3 whereas the xylose yield was greater at pH 0.5 in all experiments. This indicates that pH 0.3 was too harsh and severe sugar dehydration has taken place. The highest xylose yield of around 91% was achieved at a temperature of 140°C, a residence time of 20 min and a pH of 0.5.

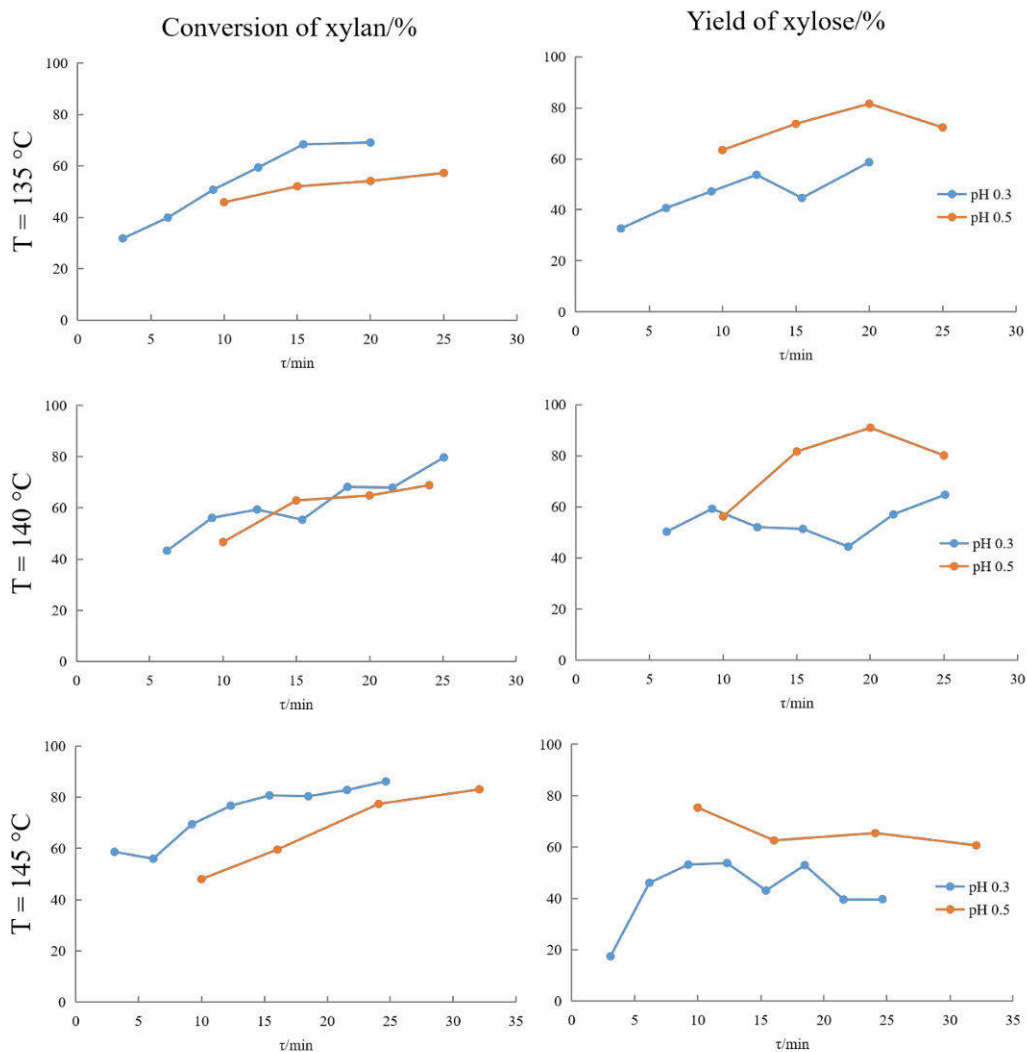


Figure 37. Influence of pH on the conversion of xylan (left) and yield of xylose (right) of experiments performed with 2 g/L solution at different temperatures and residence times.

3.3.4 Residence time distribution

In order to evaluate the residence time distribution (RTD) and thus investigate the flow regime in the reactor with the current packing, step experiments were performed with NaCl as the tracer. The response at the outlet of the reactor was determined by measuring the conductivity of the solution. The reactor was first flushed with distilled water and then the water was replaced by a

NaCl solution. Three different concentrations (1 g/L, 2 g/L and 4 g/L) were tested. The time to start pumping the NaCl solution was set to time 0. The conductivity was determined directly after the reactor, at least every ten seconds. A flow rate corresponding to a mean residence time of 20 min was employed in all experiments. The results were shown in Figure 38.

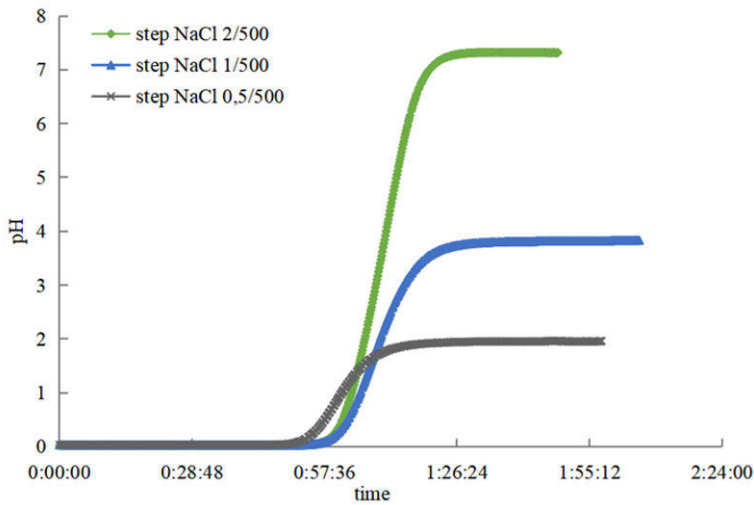


Figure 38. Conductivity as a function of time on stream in a step response experiment at a mean residence time of 20 min.

It was indicated that about 1.5 hours was required until the reactor was filled with the NaCl solution and the output concentration was stabilized. However, the volume of the piping before the reactor inlet was also taken into account. Assuming a laminar flow, the total volume from the substrate container to the outlet of the reactor could be estimated by Equation 30 based on the average half-life, which was determined to be 4023 s, and the flow rate (0.594 mL/min).

$$V_{reactor\ system} = t_{c\ 1/2} * \dot{V} \quad (30)$$

The volume of the entire reactor system before the outlet was about 40 mL. Since the outlet responses were very symmetrical, it was assumed that no dead zone existed in the reactor. In order to study the flow inside the reactor, the Peclet number was calculated according to the following equations:

$$Pe = \frac{uL}{D_z} \quad (31)$$

$$u = \frac{Q}{a\varepsilon_v} \quad (32)$$

$$\varepsilon_v = \frac{V_{liquid}}{V_{total}} \quad (33)$$

$$F(t) = \frac{1}{2} \left(1 - \operatorname{erf} \left(\frac{L - ut}{(4D_z t)^{0.5}} \right) \right) \quad (34)$$

where u was the superficial velocity, L the length of the reactor and D_z the axial dispersion coefficient. Q was defined as the flow rate, a was the cross-sectional area and ε_v was the void fraction.

Since, $F(t)$ can only obtain values between 0 and 1, the measured conductivities were divided by the maximal conductivity in the relative experiment and an average response was calculated based on the three measurements. The volume of the empty reactor was 24 mL and the displacement measurements implied that the free liquid volume after packing was 12 mL. Based on it, the volume of piping before the reactor inlet was determined. Accordingly, the residence time distribution in the reactor was calculated by subtracting the time it took for the tracer liquid to flow through the piping. The $F(t)$ function (Equation 34) was fitted to the experimental data by adjusting the D_z value, as shown in Figure 39.

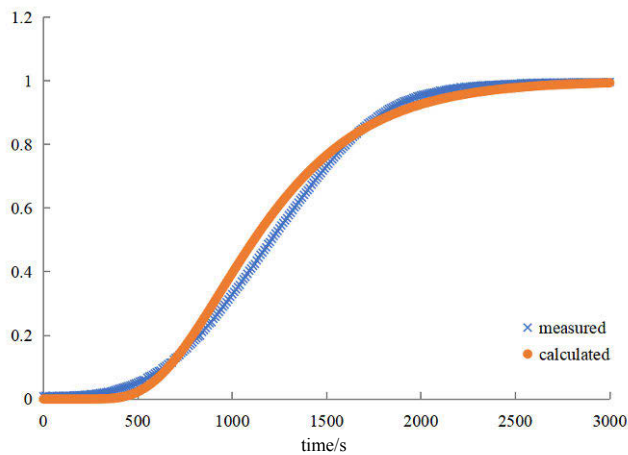


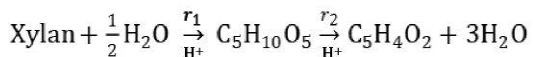
Figure 39. Measured data compared to calculated data by modelling.

The minimal possible $\sum(\Delta F(t))^2$ with adjusting was 12.257 with a D_z of 1.059×10^{-6} m²/s. Therefore, the Peclet number was calculated to be 12.1, which showed that significant turbulence was present inside the reactor despite the rather low flow rate caused by the packing.

3.3.5 Mathematical modelling

The mathematical model for the continuous reactor experiments was developed based on the data previously obtained in batch reactor experiments. The Peclet number in the current experiments was surprisingly high (~ 12), which indicated rather turbulent conditions due to the mixing effect of the reactor packing, despite the low flow rates. Moreover, the diffusion rate of the bulky xylan molecules was slower than that of the salt (NaCl) used as a tracer, which led to an even higher Peclet number than 12 for the xylan solution in practice. Even though the flow cannot be considered as complete plug flow, based on the rather high Peclet number and for the sake of simplicity, the mean residence time was used in the mathematical modelling. The model was based on the monomers formed, and thus, the formation of oligomers was neglected, even though dimers, trimers and tetramers were formed as intermediates according to the GC results. In addition, the dehydration step was included in the model.

The overall reaction can be described by a two-step consecutive reaction pathway



The reactions were considered irreversible and first order as in the modelling developed for batch reactor experiments.

The overall mass balance after implementing the rate equations (Equations 19, 20) and a modified Arrhenius equation (Equation 21) was then expressed as:

$$\frac{dc_{xylan}}{d\tau} = -k_{01} \exp\left(-\frac{E_{a1}}{R\theta}\right) c_{H^+} c_{xylan} \quad (35)$$

$$\frac{dc_{xylose}}{d\tau} = k_{01} \exp\left(-\frac{E_{a1}}{R\theta}\right) c_{H^+} c_{xylan} - k_{02} \exp\left(-\frac{E_{a2}}{R\theta}\right) c_{H^+} c_{xylose} \quad (36)$$

$$\frac{dc_{degr.}}{d\tau} = k_{02} \exp\left(-\frac{E_{a2}}{R\theta}\right) c_{H^+} c_{xylose} \quad (37)$$

where k_{01} is the pre-exponential factor, E_a the activation energy and R the universal gas constant, c_{H^+} the concentration of the protons calculated based on the number of sulfonic acid sites in the catalyst, and θ the modified temperature defined in Equation 22, in which T_{ref} was 137°C.

For the kinetic parameter estimation, a non-linear regression analysis that included parts of the experimental data was utilized. The model consisting of a system of ODEs was solved in the MODEST software. The sum of residual squares Q was calculated according to Equation 26 and minimized by the Simplex-Levenberg-Marquard method.

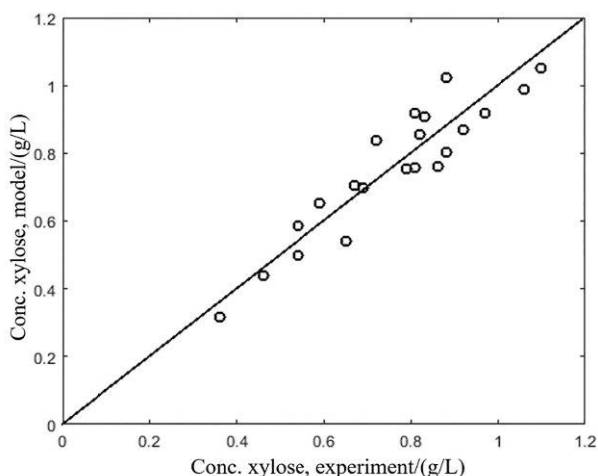


Figure 40. Fit of the model (y-axis) to the experimental data points (x-axis) of the concentration of xylose.

The fit of the model to the experimental data was shown in Figure 40. The parameters obtained in the modelling were listed in Table 7.

Table 7. Parameters after the final modelling approach.

Parameter	Value		Est. relative standard error %
k_1	0.138	L	4.3
k_2	0.0382	$\frac{\text{mol}}{\text{min}}$	8.1
E_{a1}	205	$\frac{\text{kJ}}{\text{mol}}$	6.0
E_{a2}	97.1	$\frac{\text{kJ}}{\text{mol}}$	19.6

The contour plots (Figure 41) showed that the correlation of the parameters was low and that they were well defined.

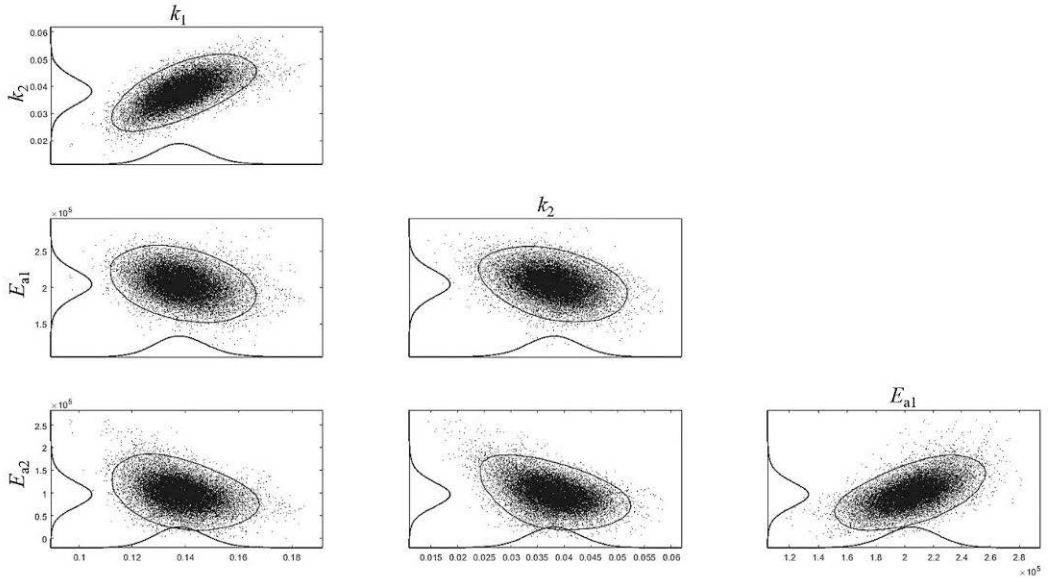


Figure 41. Contour plots of the correlation of the parameters.

3.4 One flow through hydrolysis and hydrogenation of semi-industrial hemicellulose to sugar alcohols in continuous reactor

Part of this chapter is adapted from the post print of the following article:

X. Lu, P. Junghans, S. Weckesser, J. Wärnå, G. Hilpmann, R. Lange, H. Trajano, K. Eränen, L. Estel, S. Leveneur, H. Grénman. One flow through hydrolysis and hydrogenation of semi-industrial xylan from birch (*betula pendula*) in a continuous reactor – kinetics and modelling. *Chemical Engineering and Processing - Process Intensification*, 2021, **169**, 108614.

Link: <https://doi.org/10.1016/j.cep.2021.108614>

Further permissions related to the material excerpted should be directed to the Elsevier. Copyright © 2021 Elsevier B.V. or its licensors or contributors.

The xylose produced by the acidic hydrolysis can be further hydrogenated into its corresponding C5 sugar alcohol, i.e., xylitol, which is one of the most valuable renewable chemicals for commerce. According to the previous research on the hydrolysis of xylan and hydrogenation of xylose (Figure 42), it is possible to perform a consecutive hydrolysis and hydrogenation process in one flow through in a continuous reactor to produce xylitol directly from hemicellulose, since the optimal operation temperatures and kinetics of the two reactions were very similar. Thus, the feasibility of the process was examined by conducting a set of experiments using Dowex 50WX2-100 as the hydrolyzing catalyst in the first catalyst bed and ruthenium (0.7%) on activated carbon for the hydrogenation in the second catalyst bed. The influence of several reaction parameters on the kinetics was investigated and a mathematical model was developed to express this consecutive hydrolysis and hydrogenation process. Some of the experiments were repeated three times and the relative standard deviation was determined to be within 0.1-1.5%. Based on the previous measurement of the continuous reactor used for the xylan hydrolysis, the free liquid volume accounted for around 50% of the entire reactor after filling. This value was also utilized to calculate the retention times at different liquid flow rates when performing the consecutive hydrolysis-hydrogenation experiments.

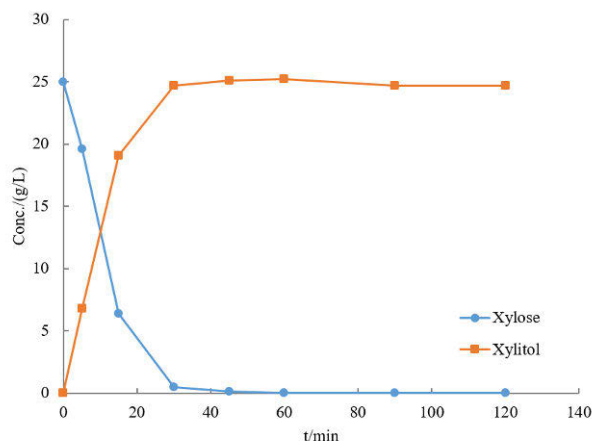


Figure 42. Hydrogenation of 25 g/L xylose to xylitol with Ru/C catalyst. Reaction conditions: 120°C, 20 bar H₂ (total pressure), 1400 rpm.

3.4.1 Influence of temperature

The effect of temperature on the yields of main products (xylose and xylitol) was studied. The H₂ pressure was kept constant at 20 bar during the whole process and a liquid flow rate of 0.1 mL/min was employed to ensure sufficient contact time between the reactants and the catalyst beds. At this flow rate, the total residence time in the reactor was 36.3 min, of which the residence times in the hydrolysis and hydrogenation catalyst beds were calculated to be 11.2 min and 5.5 min, respectively.

As shown in Figure 43, the yield of xylitol increased from 77% to 90% with a temperature rise from 130°C to 140°C, which demonstrated that elevated temperatures promoted the hydrolysis and hydrogenation significantly. In addition, less sugar degradation, i.e., dehydration was observed compared to the previously investigated hydrolysis processes where oxygen was present in the reaction mixture. It seemed plausible, that the reductive atmosphere and rapid hydrogenation of the monosaccharides after hydrolysis promoted the selectivity towards the target product and reduced the amount of undesired dehydration. Almost all of the xylose was hydrogenated as only very low concentrations, a few percent, of xylose was detected in the liquid product. The high yield of xylitol also confirmed that the substrate was effectively hydrolyzed to xylose under the selected experimental conditions.

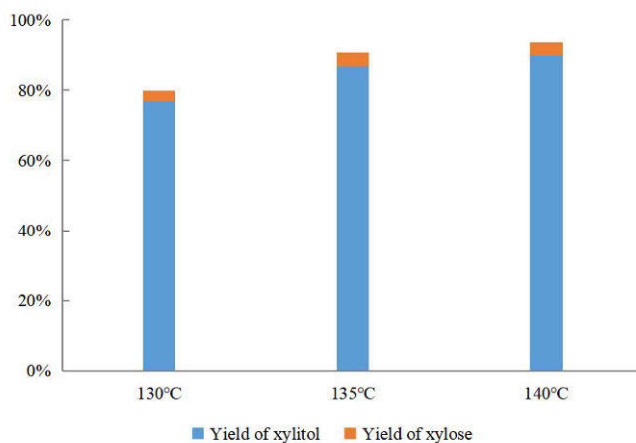


Figure 43. Influence of temperature on the xylose and xylitol yields for experiments performed at a flow rate of 0.1 mL/min under 20 bar H₂.

3.4.2 Influence of flow rate

The consecutive hydrolysis and hydrogenation experiments were carried out at different flow rates in order to evaluate how the mean residence time influenced the reaction kinetics.

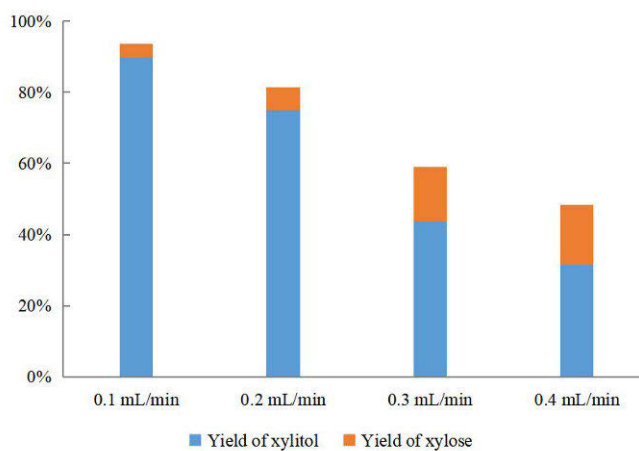


Figure 44. Influence of flow rate on the xylose and xylitol yields for experiments performed at 140°C under 20 bar H₂.

As can be observed in Figure 44, there was a significant decrease in the xylitol yield, only 31% xylitol was detected in the final product when the highest flow rate of 0.4 mL/min, which corresponded to a total residence time of 9.075 min (2.8 min for hydrolysis and 1.375 min for hydrogenation), was used. The xylan conversion was also found to decrease as the flow rate increased four fold, leaving 36% of the substrate unreacted. It can be concluded, that the residence time significantly affected the kinetics of both hydrolysis of xylan and hydrogenation of xylose. On the other hand, more xylose was produced by increasing the flow rate, which demonstrated that the hydrogenation step was more sensitive to the change in flow rate.

3.4.3 Influence of hydrogen pressure

Higher hydrogen pressures were also tested in order to see if the xylitol yield could be further enhanced by increasing the hydrogen concentration in liquid phase. A flow rate of 0.2 mL/min, corresponding to a total residence time of 18.15 min, of which 5.6 min were rationed for hydrolysis and 2.75 min hydrogenation, was applied to lower the yield and make the influence in kinetics more visible. As shown in Figure 45, no gain could be obtained by increasing the hydrogen pressure, indicating that the catalyst surface was already saturated with hydrogen at a pressure of 20 bar.

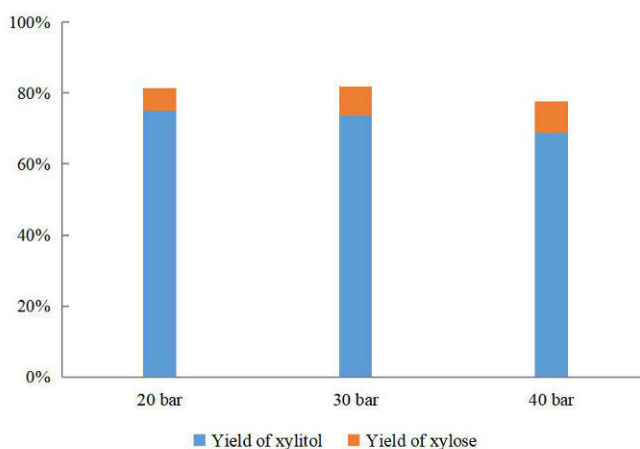
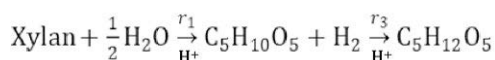


Figure 45. Influence of hydrogen pressure on the xylose and xylitol yields for experiments performed at 140°C and a flow rate of 0.2 mL/min.

3.4.4 Mathematical modelling

In the modelling approach chosen for the consecutive hydrolysis and hydrogenation processes, the hydrolysis step was calculated according to equations presented in previous chapters, while the dehydration of monosaccharides was excluded, since it was shown to be greatly suppressed by the reductive conditions. Concentrations were calculated as mol/L to take into account the stoichiometry in the consecutive reactions. When considering irreversible hydrolysis and hydrogenation steps, the overall reaction scheme becomes:



The xylose concentration from the hydrolysis catalyst bed, the amount of catalyst and the pressure of hydrogen were incorporated in the hydrogenation step. The adsorption of xylose and hydrogen were also taken into account in the model. The overall mass balance are expressed as:

$$\frac{dc_{xylose}}{d\tau} = r_1 - r_3 = k_1 c_{\text{H}^+} c_{\text{xylan}} - \frac{k_3 c_{xylose} p_{\text{H}_2}}{1 + K_{xylose} c_{xylose} + K_{\text{H}_2} p_{\text{H}_2}} \quad (38)$$

$$\frac{dc_{xylitol}}{d\tau} = r_3 = \frac{k_3 c_{xylose} p_{\text{H}_2}}{1 + K_{xylose} c_{xylose} + K_{\text{H}_2} p_{\text{H}_2}} \quad (39)$$

The results showed that the inclusion of adsorption to the model did not improve the model fit nor provide any statistical advantage, thus the model could be further simplified to

$$\frac{dc_{xylitol}}{d\tau} = r_3 = k_3 c_{xylose} p_{\text{H}_2} \quad (40)$$

The fit of the model ($R^2=98.7\%$) to the experimental data was shown in Figure 46. The parameters obtained in the modelling were listed in Table 8. The contour plots (Figure 47) showed that the correlation of the parameters was low and that they were well defined.

The average degree of depolymerization was estimated based on the kinetics via the stoichiometry observed in the analysis. The estimated average DP became 24, which was lower than that obtained from SEC-MALS analysis. The standard error of the estimated DP was very low, being only 4.3%.

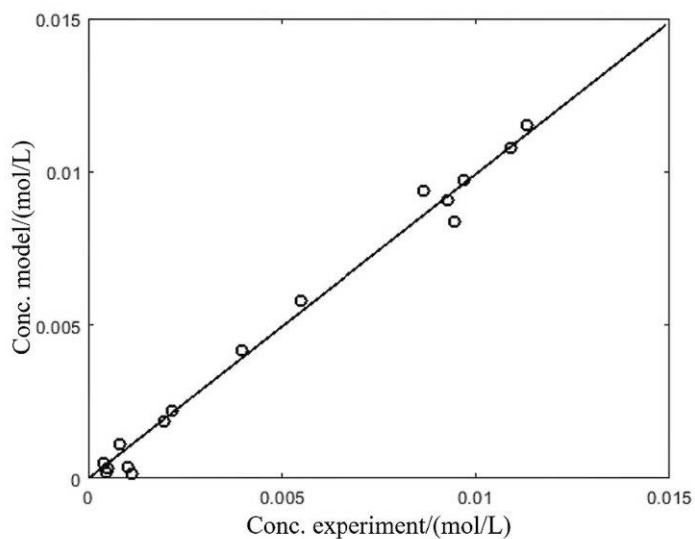


Figure 46. Fit of the model (y-axis) to the experimental data points (x-axis) of the concentrations of xylose and xylitol.

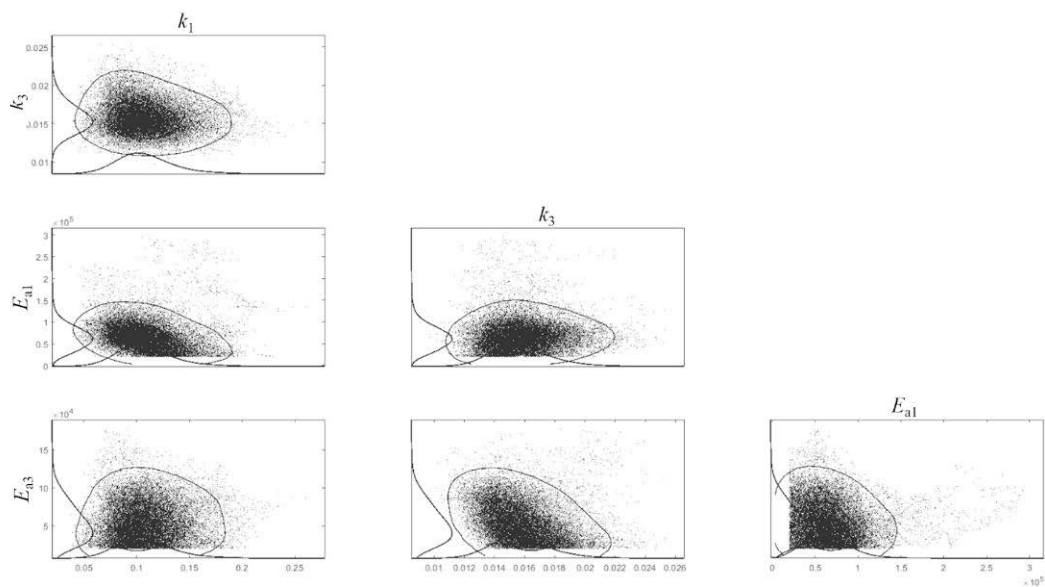


Figure 47. Contour plots of the correlation of the parameters.

Table 8. Parameters after the final modelling approach.

Parameter	Value		Est. relative standard error %
k_1	0.101	$\frac{\text{L}}{\text{mol} \cdot \text{min}}$	13.1
k_3	0.0157		10.9
E_{a1}	68.3	$\frac{\text{kJ}}{\text{mol}}$	27.5
E_{a3}	43.7		71.2

3.5 Specific heat capacity measurement for typical supports used for heterogeneous catalysts

Part of this chapter is adapted from the post print of the following article:

X. Lu, Y. Wang, L. Estel, N. Kumar, H. Grénman, S. Leveneur. Evolution of specific heat capacity with temperature for typical supports used for heterogeneous catalysts. *Processes*, 2020, **8**, 911.

Link: <https://doi.org/10.3390/pr8080911>

Further permissions related to the material excerpted should be directed to the MDPI. Copyright © 2020 MDPI (Basel, Switzerland).

Catalyst is widely used in biorefinery. The specific heat capacity of the catalyst employed is an important parameter when calculating the energy balance. The specific heat capacity of numerous heterogeneous catalysts that can be applied to biorefinery processes were measured with a C80 micro-calorimeter. The C_p measurement on each catalytic material was repeated three times without replacing the sample in between, giving a maximum standard error of 1.79%. Figure 48 showed the C_p values as a function of T . It was observed that the C_p of different catalytic materials at the same temperature differed greatly, which would significantly influence the temperature profile under a non-isothermal condition. In addition, the variation of C_p with temperature was not similar, although in general, the C_p was higher at elevated temperatures.

The C_p of alumina silicate materials are influenced by both silica and alumina. However, no clear relationship between the C_p value and the $\text{SiO}_2/\text{Al}_2\text{O}_3$ ratio was observed for the studied materials. The C_p of H-Beta-38 and SiO_2 were observed to be more sensitive to a temperature change compared to other materials, whereas the C_p of TiO_2 was almost independent of temperature. The C_p values measured for both activated carbon and alumina were found to be higher than the values reported previously [48]. This was probably due to the use of different instruments employing different measuring mechanisms. Moreover, the great difference in C_p values between the activated carbon and graphite can also be the result of difference in crystal

morphology of the materials. Further studies are required to explore the influence of different parameters on the heat capacity of these catalytic materials.

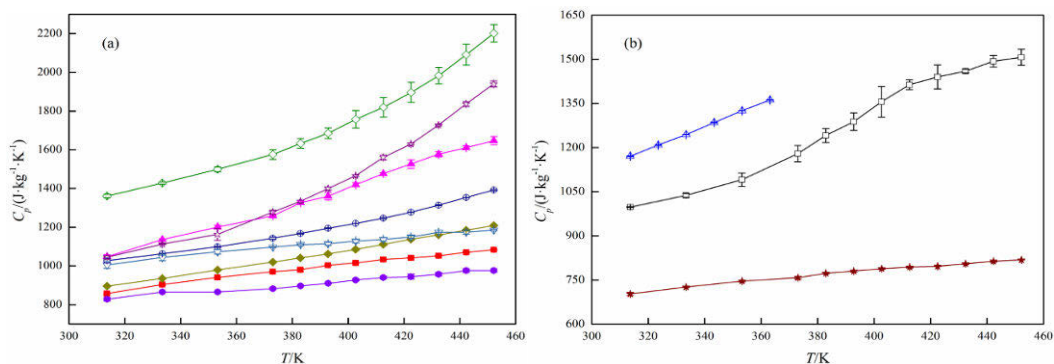


Figure 48. C_p values of (a) catalytic materials containing alumina or silica, and (b) other catalytic materials as a function of temperature. □, activated carbon; ■, Al_2O_3 ; △, amberlite IR120, H-form; ▲, H-Beta-25; ◇, H-Beta-38; ◆, H-Y-60; ○, H-ZSM-5-23; ●, H-ZSM-5-280; ☆, SiO_2 ; ★, TiO_2 ; ▽, zeolite 13X.

The evolution of C_p with T was shown to follow a polynomial dependence of the second-order [49]. The experimental data were correlated with Equation 41 and the fitting results were illustrated in Table 9. The standard errors of the fitting parameters were calculated with Athena Visual Studio [50], providing a confidence interval of 0.95.

$$C_p(T) = C_p(T_{ref}) + A \times (T - T_{ref}) + B \times (T^2 - T_{ref}^2) \quad (41)$$

where T and T_{ref} represent the measurement temperature and the reference temperature, A and B are constants determined by the inherent properties of the studied material.

As shown in Table 9, satisfactory correlation was achieved for each sample, with a determination coefficient above 97%, although the estimated errors for the correlation parameters were not always low. A linear relationship between C_p and T was observed for Amberlite IR120, H-Beta-25, and H-ZSM-5-280 in the measured temperature range, hence the equations can be simplified by implementing $B = 0$ for these materials.

Table 9. Correlation results of C_p data for different catalytic materials with Equation 41.

	T_{ref}/K	$C_p(T_{ref})/(\text{J}\cdot\text{kg}^{-1}\cdot\text{K}^{-1})$	$A/(\text{J}\cdot\text{kg}^{-1}\cdot\text{K}^{-2})$	Estimated Error of $A/(\text{J}\cdot\text{kg}^{-1}\cdot\text{K}^{-2})$	$B/(\text{J}\cdot\text{kg}^{-1}\cdot\text{K}^{-3})$	Estimated Error of $B/(\text{J}\cdot\text{kg}^{-1}\cdot\text{K}^{-3})$	R^2
Activated carbon	392.74	1288.34	2.89	5.57	0.0016	0.0072	0.9992
Al ₂ O ₃	392.73	1003.09	4.37	0.79	-0.0036	0.0010	0.9971
Amberlite IR120, H-form	353.21	1325.63	3.94	0.09			0.9992
H-Beta-25	402.67	1419.67	4.42	0.28			0.9910
H-Beta-38	392.81	1685.38	-19.39	2.47	0.0329	0.0032	0.9981
H-Y-60	372.97	1019.52	0.42	0.35	0.0024	0.0004	0.9998
H-ZSM-5-23	392.77	1194.68	-3.87	0.75	0.0084	0.0010	0.9991
H-ZSM-5-280	392.79	910.64	1.08	0.12			0.9729
SiO ₂	392.75	1399.71	-1.94	1.58	0.0337	0.0021	0.9994
TiO ₂	402.66	788.29	2.92	0.62	-0.0027	0.0008	0.9944
Zeolite 13X	373.00	1097.44	3.44	1.24	-0.0029	0.0016	0.9907

4 Conclusions and perspectives

Various chemical catalysis technologies were employed to valorize different fractions of lignocellulosic biomass, specifically Finnish silver birch, produced by a novel semi-industrial biorefinery process.

Reductive catalytic depolymerization was performed on the lignin fraction using Ru/C, Pd/C and Ni/Al₂O₃ catalysts. The macromolecules in the substrate were gradually fragmented into monomers and dimers with a continuous decline in the average molecular weight over reaction time, showing a consecutive reaction pathway. The catalyst and hydrogen were proven to be essential to achieve selective depolymerization and high stability and yield of the lignin oil product. The reaction kinetics were strongly promoted by elevated temperature displaying rather high activation energy. The reaction medium, consisting of organic solvent and/or water, significantly influenced the reaction products, while ethanol-water and methanol-water mixtures led to the highest yields. A maximum of 98% mono- to tetramers were collected in the liquid phase products, where monomers and dimers dominated (85%). Gaseous products, mainly CH₄, CO₂ and short alkanes were also formed under the studied conditions.

Heterogeneously catalyzed hydrolysis of the xylan fraction was first studied in a batch reactor. It can be concluded, that a semi-industrial xylan produced in a novel sustainable process could be efficiently hydrolyzed by the commercial acidic catalyst Dowex 50WX2-100. It was observed, that the the sugars also underwent dehydration, which significantly affected the obtainable yield of xylose. The design of experimental conditions was therefore very important for optimization. The highest yield of monosaccharides (76%) was achieved at 137°C and pH 0.75. Kinetic modelling was performed on the data from batch reactor experiments, taking into account the dehydration of sugar products and an excellent fit was obtained.

A continuous process was developed for the acidic hydrolysis of xylan fraction from Finnish silver birch. The heterogeneous catalyst and preliminary reaction conditions were chosen based on the results of batch reactor experiments. Finding a compromise between the reaction kinetics of hydrolysis and unwanted side reactions to obtain the highest possible monosaccharide yield was the key to the process optimization and intensification. The highest yield of above 90% was achieved by processing 2 g/L xylan solution at 140°C, pH 0.5 and a residence time of 20 min. It

was indicated that severer conditions, such as higher temperature and lower pH, promoted the sugar degradation more significantly.

The semi-industrial xylan was then processed in another continuous reactor equipped with two catalyst beds for producing sugar alcohols in a one flow through hydrolysis and hydrogenation process. Dowex 50WX2-100 was chosen to catalyze hydrolysis and Ru/C for the hydrogenation. The substrate underwent hydrolysis and hydrogenation and converted the xylan into xylitol with high yield. An elevated temperature and a low liquid flow rate was proven to be favorable to obtaining satisfactory yield and selectivity. The most efficient conversion was achieved at 140°C with 0.1 mL/min liquid and 20 bar H₂ flowing through, converting 82% of xylan and producing 90% of xylitol based on the initial xylose concentration in the substrate. It was concluded, that the reductive conditions employed and the fast hydrogenation of monosaccharides prevented the undesired dehydration of the sugars. The one flow through reactor system enabled significant process intensification, as only one reactor was needed and higher selectivity and yield towards xylitol was achieved compared to conducting the two reaction steps separately. In addition, a kinetic model was developed and a good fit of the model to the experimental data was obtained.

Moreover, the specific heat capacities of numerous catalytic supports that were employed in the current work and can be employed in the valorization of different fractions of biomass were determined with a Tian-Calvet micro-calorimeter. The temperature dependence of the specific heat capacity of each catalytic material was studied and successfully expressed by a polynomial equation. These data are highly important in developing and scaling up efficient and safe chemical processes.

To conclude, the special semi-industrial lignin and hemicellulose fractions were successfully valorized to desired products in high yields employing different technical means with commercial catalysts. The work contributes to developing novel and sustainable biorefinery processes, which utilizes efficiently all the fractions of the woody biomass. The overall process is very well aligned with the principles of green engineering and chemistry, as almost 100% of the renewable feedstock is utilized for products and recirculation, and high energy efficiency was achieved by implementing aqueous based systems.

However, further studies are required on each topic. For example, the specific heat capacity of other catalytic materials and raw materials in biorefinery need to be measured to fill the gap in

knowledge. The relationships between heat capacities and the structure/properties of these materials are important information in industry. The catalyst stability tests are required for long term applications. Moreover, the valorization of different biomass fractions should be investigated in continuous reactor more systematically, before scaling up. In order to realize the industrial application of the process, experimental data under non-isothermal conditions are also required. The corresponding thermal risk analysis should be performed, taking into account the specific heat capacities of all reactants and catalytic materials.

Notation

A, B	Parameters in the specific heat capacity equation
a	Cross-sectional area (m^2)
C_p	Specific heat capacities ($\text{J}\cdot\text{kg}^{-1}\cdot\text{K}^{-1}$)
c	Concentration (g/L)
c_i^0	Initial concentrations of component i (g/L)
d	Diameter of the reactor (cm)
DP	Degree of depolymerization
DSC	Differential scanning calorimetry
D_z	Axial dispersion coefficient (m^2/s)
E_a	Activation energy (kJ/mol)
EtOH	Ethanol
GVL	γ -valerolactone
HPSEC	High-pressure size-exclusion chromatography
K	Adsorption coefficient
k	Conversion dependent pre-exponential factor (min^{-1})
k_0	Pre-exponential factor (min^{-1})
$k_{01/02}$	Pre-exponential factors ($\text{L}\cdot\text{mol}^{-1}\cdot\text{min}^{-1}$)
k_∞	Pre-exponential factor at the end of the reaction (min^{-1})
L	Length of the reactor (m)
MeOH	Methanol
M_w	Weight average molecular weight (g/mol)
m	Mass (g)
P	Pressure (Pa)
Q	Volumetric flow rate (m^3/s)
Q	Sum of residual squares
Q_c	Total heat absorbed in the presence of a sample
Q_b	Total heat absorbed in the absence of a sample

R	General gas constant ($\text{J}\cdot\text{mol}^{-1}\cdot\text{K}^{-1}$)
RCD	Reductive catalytic depolymerization
RTD	Residence time distribution
r	Reaction rate
$t_{c\ 1/2}$	Half-life (s)
T	Temperature (K)
T_{ref}	Reference temperature (K)
ΔT	Temperature difference (K)
TEC	Total ion exchange capacity (meq/g)
THF	Tetrahydrofuran
u	Superficial velocity (m/s)
V	Volume (mL)
\dot{V}	Volumetric flow rate (mL/min)
x_i	Content of component i (%)
X	Conversion (%)
Y	Yield (%)
α, β	Parameters in the rate equation
ε_v	Void fraction
θ	Modified temperature (K)
ρ	Density (g/mL)
ρ_b	Bulk density (g/mL)
τ	Residence time (min)

Subscripts and superscripts

<i>cat.</i>	Catalyst
<i>degr.</i>	Degradation product
<i>exp</i>	Experimental data
<i>est</i>	Estimated data by modelling

Acknowledgments

This work was conducted as a double degree project (cotutelle) between the Laboratory of Industrial Chemistry and Reaction Engineering (TKR) at Åbo Akademi University (Finland) and the Laboratoire de Sécurité des Procédés Chimiques (LSPC) at Institut National des Sciences Appliquées (INSA) de Rouen Normandie (France). The study has been performed in the framework of the AMED project financed with the support from the European Union within the European Regional Development Fund (ERDF) and from the Regional Council of Normandie. The China Scholarship Council: Cooperation Program with the UTs (Universités de technologie) and INSAs is gratefully acknowledged for financial support as is the Åbo Akademi University strategic profiling area Technologies for a Sustainable Future. CH-Bioforce is gratefully acknowledged for supplying the raw materials required for the experiments.

References

- [1] M. Fitz Patrick, P. Champagne, M. F. Cunningham, R. A. Whitney. *Bioresour. Technol.*, 2010, **101**, 8915–8922.
- [2] M. Moshkelani, M. Marinova, M. Perrier, J. Paris. *Appl. Therm. Eng.*, 2013, **50**, 1427–1436.
- [3] X. Kang, Y. Wang, S. Wang, X. Song. *Carbohydr. Polym.*, 2021, **255**, 117391.
- [4] O. Ajao, M. Marinova, O. Savadogo, J. Paris. *Ind. Crops Prod.*, 2018, **126**, 250–260.
- [5] M. Fache, B. Boutevin and S. Caillol. *ACS Sustainable Chem. Eng.*, 2016, **4**, 35–46.
- [6] B. M. Upton and A. M. Kasko. *Chem. Rev.*, 2016, **116**, 2275–2306.
- [7] S. Laurichesse and L. Avérous. *Prog. Polym. Sci.*, 2014, **39**, 1266–1290.
- [8] J. H. Lora and W. G. Glasser. *J. Polym. Environ.*, 2020, **10**, 39–48.
- [9] S. Saka, H.-J. Bae. Chapter 11 - Secondary Xylem for Bioconversion, ed. Y. S. Kim, R. Funada and A. P. Singh, *Secondary Xylem Biology*, Academic Press, 2016, pp. 213-231.
- [10] S. Von Schoultz. Method for extracting biomass. *WO 2014/009604*, 2014.
- [11] S. Von Schoultz. Method for extracting lignin. *WO 2015/104460*, 2015.
- [12] H. Wang, H. Ben, H. Ruan, L. Zhang, Y. Pu, M. Feng, A. J. Ragauskas and B. Yang. *ACS Sustainable Chem. Eng.*, 2017, **5**, 1824–1830.
- [13] E. M. Anderson, M. L. Stone, M. J. Hülsey, G. T. Beckham and Y. Román-Leshkov. *ACS Sustainable Chem. Eng.*, 2018, **6**, 7951–7959.
- [14] B. M. Harahap. *Jurnal Keteknikan Pertanian Tropis dan Biosistem*, 2020, **8(2)**, 107-124.
- [15] B. T. Kusema, C. Xu, P. Mäki-Arvela, S. Willför, B. Holmbom, T. Salmi, D. Y. Murzin. *Int. J. Chem. React. Eng.*, 2010, **8(1)**.
- [16] J. P. Lange, E. van der Heide, J. van Buijtenen, R. Price. *ChemSusChem*, 2012, **5**, 150–166.
- [17] A. Sharples. *Trans. Faraday Soc.*, 1957, **53**, 1003–1013.
- [18] M. Cuevas, J. García, G. Hodaifa, S. Sánchez. *Ind. Crops Prod.*, 2015, **70**, 100–106.

- [19] T. Hornbogen and J. Schaaf. Hydrolysis of birch hemicelluloses by heterogeneous acid catalysts, 2017.
- [20] A. Pérez Nebreda, V. Russo, M. Di Serio, T. Salmi, H. Grénman. *Chem. Eng. Sci.*, 2019, **195**, 758–766.
- [21] A. Pérez Nebreda, H. Grénman, P. Mäki-Arvela, K. Eränen, J. Hemming, S. Willför, D. Y. Murzin, T. Salmi. *Holzforschung*, 2016, **70**, 187–194.
- [22] M. Herskowitz. *Chem. Eng. Sci.*, 1985, **40**, 1309–1311.
- [23] H. Ling, K. Cheng, J. Ge, W. Ping. *Nat. Biotechnol.*, 2011, **28**, 673–678.
- [24] A. P. Tathod, P. L. Dhepe, *Green Chem.*, 2014, **16**, 4944–4954.
- [25] J. Holladay, J. Bozell, J. White, D. Johnson. Top value-added chemicals from biomass. DOE Report PNNL 16983 2007.
- [26] P. Sudarsanam, R. Zhong, S. V. D. Bosch, S. M. Coman, V. I. Parvulescu, B. F. Sels. *Chem. Soc. Rev.*, 2018, **47**, 8349–8402.
- [27] F. Chen, T. Zhao, J. Liang, W. Cao, Y. Jiang, X. Xu. *J. Am. Oil Chem. Soc.*, 2019, **96**, 1011–1018.
- [28] A. Kuprava, I. Saenko, O. Fabrichnaya. *Calphad*, 2020, **68**, 101745.
- [29] C. Quick, J. Schawe, P. Uggowitzer, S. Pogatscher. *Thermochim. Acta*, 2019, **677**, 12–20.
- [30] T. L. Reichmann, D. Li, D. M. Cupid. *Phys. Chem. Chem. Phys.*, 2018, **20**, 22856–22866.
- [31] H. Niu, S. Chen, S. Jin, B. Li, X. Li, J. Wang, X. Ma, F. Bao, L. Li. *J. Therm. Anal. Calorim.*, 2017, **131**, 3193–3199.
- [32] L. Lagerquist, A. Pranovich, A. Smeds, S. von Schoultz, L. Vähäsalo, J. Rahkila, I. Kilpeläinen, T. Tamminen, S. Willför and P. Eklund. *Ind. Crops Prod.*, 2018, **111**, 306–316.
- [33] V. Molinari, G. Clavel, M. Graglia, M. Antonietti, and D. Esposito. *ACS Catal.*, 2016, **6**, 1663–1670.
- [34] K. M. Isa, T. A. T. Abdullah and U. F. M. Ali. *Renewable Sustainable Energy Rev.*, 2018, **81**, 1259–1268.

- [35] W. Schutyser, T. Renders, S. Van den Bosch, S.-F. Koelewijn, G. T. Beckham and B. F. Sels. *Chem. Soc. Rev.*, 2018, **47**, 852–908.
- [36] X. Ouyang, X. Huang, J. Zhu, M. D. Boot and E. J. M. Hensen. *ACS Sustainable Chem. Eng.*, 2019, **7**, 13764–13773.
- [37] J. Long, Y. Xu, T. Wang, Z. Yuan, R. Shu, Q. Zhang and L. Ma. *Appl. Energy*, 2015, **141**, 70–79.
- [38] J. V. Vermaas, M. F. Crowley and G. T. Beckham. *ACS Sustainable Chem. Eng.*, 2020, **8**, 17839–17850.
- [39] H. Konnerth, J. Zhang, D. Ma, M. H. G. Precht and N. Yan. *Chem. Eng. Sci.*, 2015, **123**, 155–163.
- [40] S. Chu, A. V. Subrahmanyam and G. W. Huber. *Green Chem.*, 2013, **15**, 125–136.
- [41] J. Y. Kim, J. Park, H. Hwang, J. K. Kim, I. K. Song and J. W. Choi. *J. Anal. Appl. Pyrolysis*, 2015, **113**, 99–106.
- [42] X. Dou, X. Jiang, W. Li, C. Zhu, Q. Liu, Q. Lu, X. Zheng, H. Chang and H. Jameel. *Appl. Catal., B*, 2020, **268**, 118429.
- [43] C. S. Lancefield, H. L. J. Wienk, R. Boelens, B. M. Weckhuysen and P. C. A. Bruijninx. *Chem. Sci.*, 2018, **9**, 6348–6360.
- [44] A. P. Nebreda, T. Salmi, D. Murzin and H. Grénman. *J. Chem. Technol. Biotechnol.*, 2018, **93**, 224–232.
- [45] A. P. Nebreda, V. Russo, M. Di Serio, K. Eränen, D. Murzin, T. Salmi and H. Grénman. *J. Chem. Technol. Biotechnol.*, 2019, **94**, 418–425.
- [46] F. Delbecq, Y. Wang, A. Muralidhara, K. El Ouardi, G. Marlair and C. Len. *Front. Chem.*, 2018, **6**, 146.
- [47] A. Beckendorff, A. Lamp and M. Kaltschmitt. *Biomass Conv. Bioref.*, 2021, DOI: <https://doi.org/10.1007/s13399-021-01429-6>.
- [48] Z.-C. Tan, J.-B. Zhang, M. Shang-He. *J. Therm. Anal. Calorim.*, 1999, **55**, 283–289.

[49] H. Ariba, Y. Wang, C. Devouge-Boyer, R. P. Stateva, S. Leveneur. *J. Chem. Eng. Data*, 2020, **65**, 3008–3020.

[50] W. E. Stewart, M. Caracotsios. Athena Visual Studio. Available online: www.athenavisual.com (accessed on 10 June 2020).

ISBN 978-952-12-4096-6 (printed version)
ISBN 978-952-12-4097-3 (electronic version)
ISSN 2669-8315 2670-0638 (Acta technologiae chemicae Aboensia 2021 A/4)

Painosalama, Turku/Åbo, Finland 2021